

The determining factors of hydrogen isotope offsets between plants and their source waters

Liangju Zhao¹ , Xiaohong Liu² , Ninglian Wang¹ , Adrià Barbeta³ , Yu Zhang² ,
Lucas A. Cernusak⁴  and Lixin Wang⁵ 

¹Shaanxi Key Laboratory of Earth Surface System and Environmental Carrying Capacity, College of Urban and Environmental Sciences, Northwest University, Xi'an, 710069, China;

²School of Geography and Tourism, Shaanxi Normal University, Xi'an, 710119, China; ³BEECA, Department of Evolutionary Biology, Ecology and Environmental Sciences, Universitat de Barcelona, Barcelona, Catalonia, 08007, Spain; ⁴College of Science and Engineering, James Cook University, Cairns, QLD, 4878, Australia; ⁵Department of Earth and Environmental Sciences, Indiana University Indianapolis (IUI), Indianapolis, IN 46202, USA

Summary

Authors for correspondence:
Ninglian Wang
Email: nlwang@nwu.edu.cn

Lixin Wang
Email: lxwang@iupui.edu

Received: 4 September 2023
Accepted: 22 November 2023

New Phytologist (2024) **241**: 2009–2024
doi: 10.1111/nph.19492

Key words: ecohydrology, hydrogen fractionation, hydrogen isotope offset, plant functional type, $\delta^2\text{H}$ offset correction.

- A fundamental assumption when using hydrogen and oxygen stable isotopes to understand ecohydrological processes is that no isotope fractionation occurs during plant water uptake/transport/redistribution. A growing body of evidence has indicated that hydrogen isotope fractionation occurs in certain environments or for certain plant species. However, whether the plant water source hydrogen isotope offset ($\delta^2\text{H}$ offset) is a common phenomenon and how it varies among different climates and plant functional types remains unclear.
- Here, we demonstrated the presence of positive, negative, and zero offsets based on extensive observations of 12 plant species of 635 paired stable isotopic compositions along a strong climate gradient within an inland river basin.
- Both temperature and relative humidity affected $\delta^2\text{H}$ offsets. In cool and moist environments, temperature mainly affected $\delta^2\text{H}$ offsets negatively due to its role in physiological activity. In warm and dry environments, relative humidity mainly affected $\delta^2\text{H}$ offsets, likely by impacting plant leaf stomatal conductance. These $\delta^2\text{H}$ offsets also showed substantial linkages with leaf water ^{18}O enrichment, an indicator of transpiration and evaporative demand.
- Further studies focusing on the ecophysiological and biochemical understanding of plant $\delta^2\text{H}$ dynamics under specific environments are essential for understanding regional ecohydrological processes and for conducting paleoclimate reconstructions.

Introduction

The stable isotopes of hydrogen and oxygen in plant water are commonly used in ecohydrology to assess processes such as root water uptake (Ehleringer & Dawson, 1992; Lanning *et al.*, 2020; Zhao *et al.*, 2020), the competition between different plant species for soil water (Dawson & Pate, 1996), evapotranspiration partitioning (Wang *et al.*, 2013, 2014), local moisture recycling (Peng *et al.*, 2011; Zhao *et al.*, 2019) and the hydraulic connectivity of plant transpiration, groundwater and streamflow across different scales (Wang *et al.*, 2010; Jasechko *et al.*, 2013; Evaristo *et al.*, 2015, 2017; Barbeta & Penuelas, 2017). For plant water uptake, nearly all water used by plants ultimately originates from precipitation, and this precipitation is available to plants from different pools within ecosystems. Two predominant pools are water held under tension in soils (the vadose zone) and water held under pressure in groundwater (the saturated zone). Each can be complex water storages that vary spatially and temporally in isotopic values (Sprenger *et al.*, 2016; Allen *et al.*, 2019, 2022). A key assumption in the applications of isotopes in ecohydrology is that

no isotopic fractionation occurs during root water uptake, but a growing number of studies have shown unexplained isotopic mismatches between xylem water and plant water sources. These findings challenge the assumption that no isotopic fractionation occurs during root water uptake. At first, observations of plant water source hydrogen isotopic offset (the $\delta^2\text{H}$ offset) were restricted to saline or xeric environments (Lin & Sternberg, 1992; Ellsworth & Williams, 2007). More recently, such $\delta^2\text{H}$ offsets were reported in temperate riparian forests (Barbeta *et al.*, 2019) or extremely arid regions (Zhao *et al.*, 2016) and over a range of soil types, plant species, and moisture status (Newberry *et al.*, 2017; Vargas *et al.*, 2017; Barbeta *et al.*, 2020). For example, Zhao *et al.* (2016) observed that hydrogen isotopic discrimination occurred during water transport/redistribution within *Populus euphratica* Oliv. Barbeta *et al.* (2019) reported that the estimation of plant water sources using mixing models was strongly affected by $\delta^2\text{H}$ depletion in *Fagus sylvatica* (L.) and *Quercus robur* (L.). More recently, Barbeta *et al.* (2020) found that regardless of substrate, soil, and stem water $\delta^2\text{H}$ were similar only near permanent wilting point in the temperate tree species *Fagus sylvatica* (near-zero $\delta^2\text{H}$ offset). Under

moister conditions, stem water $\delta^2\text{H}$ was $11 \pm 3\text{‰}$ more negative than soil water $\delta^2\text{H}$ (negative $\delta^2\text{H}$ offset), and under drier conditions, stem water $\delta^2\text{H}$ became progressively more enriched than soil water $\delta^2\text{H}$ (positive $\delta^2\text{H}$ offset). Evidence from experimental studies may imply that field studies (Evaristo *et al.*, 2017; Geris *et al.*, 2017; Wang *et al.*, 2017; Deurwaerder *et al.*, 2018; Oerter & Bowen, 2019) could have been affected by the $\delta^2\text{H}$ offsets. Indeed, those studies reported either more positive or negative xylem δ -values, compared to source waters. Recently, our work suggested hydrogen isotopic fractionation occurred between xylem sap and bulk stem or root water (extracted cryogenically) (Zhao *et al.*, 2016), whereas this was not observed for oxygen isotopes. Altogether, these studies suggest that isotopic fractionation during root water uptake or within-plant water transport might be more common than we thought previously.

Instead, Chen *et al.* (2020) showed recently that the measurement bias inherent in the cryogenic extraction method may be the cause of xylem ^2H depletion, and thus, *in situ* measurements (Wang *et al.*, 2012) or alternative extraction methods should overcome this issue. For instance, Barbeta *et al.* (2022) demonstrated that sap water extracted with a centrifuge from cut stems gives a much more reliable estimation of the isotopic composition of plant water source, compared to the traditional cryogenic vacuum distillation (CVD). Even though the evidence of the $\delta^2\text{H}$ offset when using CVD to extract plant water has been clearly demonstrated by controlled experiments (Vargas *et al.*, 2017; Barbeta *et al.*, 2019; Chen *et al.*, 2020), the mechanism producing such $\delta^2\text{H}$ offsets remains unclear. Therefore, the existence of $\delta^2\text{H}$ offsets in plants growing over a range of soil and climatic conditions remains largely unknown.

Given the importance of the $\delta^2\text{H}$ offsets in isotope-based research, it is imperative for us to have a better understanding of their environmental and biological controls. To achieve this goal, we conducted a basin-scale study from the upper, middle, and lower reaches of the inland Heihe River Basin (Supporting Information Fig. S1), covering a strong climate gradient to examine the spatial variability of the $\delta^2\text{H}$ offsets of all the dominant species (Tables 1 and 2). We considered the potential influence of climatic factors (e.g. temperature and relative humidity) and

plant transpiration indicators such as plant leaf water $\delta^{18}\text{O}$ (e.g. $\delta^{18}\text{O}_{\text{Leaf}}$) and the difference between $\delta^{18}\text{O}_{\text{Leaf}}$ and $\delta^{18}\text{O}_{\text{Xylem}}$ water (e.g. $\Delta^{18}\text{O}_{\text{Leaf-Xylem}}$) to indicate the enrichment in ^{18}O of leaf water above the $\delta^{18}\text{O}$ value of the source water used by plants. These indicators are useful to represent various impacts of stomatal regulation (Larcher *et al.*, 2015; Ellsworth *et al.*, 2023). We also assessed the effect of plant growth form by comparing trees, shrubs, and grasses. We further evaluated the sensitivities of the $\delta^2\text{H}$ offsets to climates, $\delta^{18}\text{O}_{\text{Leaf}}$ and $\Delta^{18}\text{O}_{\text{Leaf-Xylem}}$ (temperature and evaporative demand), and discussed their implications for plant water source identification, evapotranspiration partitioning, moisture recycling, and paleoclimate studies.

Materials and Methods

Study region

The study was conducted at the upper reaches (Qilian Mountains), the middle reaches (Linze), and the lower reaches (Ejina) of the Heihe River Basin in northwestern China (Fig. S1). The Heihe River Basin includes a semiarid region in the upper reaches, an arid transitional region in the middle reaches, and an extremely arid region in the lower reaches. We measured the stable isotope composition ($\delta^2\text{H}$ and $\delta^{18}\text{O}$) of different water pools such as precipitation, groundwater, soil water, plant xylem water, and leaf water accessed by different plant species in all reaches of the basin (Fig. S2). We also collected meteorological data including temperature and relative humidity, which varied with differing elevations (Fig. S1). For the upper reaches, we used meteorological stations located at Pailugou and Yeniugou to represent the middle mountains and the alpine region of the Qilian Mountains (Fig. S1). In Yeniugou ($38^\circ 25' \text{N}$, $99^\circ 35' \text{E}$, elevation: 3320 m asl), the long-term (1960–2012) mean annual precipitation is 416 mm, and 80% of it occurs between June and September (Fig. S1). Pailugou ($100^\circ 17' \text{N}$, $38^\circ 24' \text{E}$, elevation: 2780 m asl) lies in the middle of the Qilian Mountains. Annual precipitation averages 369 mm, and 72% of it occurs between June and September. Both areas have similar ecosystem types consisting of mountain grasslands,

Table 1 The acronyms of study regions, plant species, plant functional types, and growing environment across the Heihe River Basin.

Acronym	The full name	Region	Plant species		Region	Functional type of the species
			Acronym	The full name		
HRB	The Heihe River Basin	–	QS	Qinghai Spruce	UR	Evergreen coniferous tree
UR	The upper reaches of the HRB	–	PF	<i>Potentilla fruticosa</i> L.	UR	Deciduous broadleaf shrub
MR	The middle reaches of the HRB	–	PV	<i>Polygonum viviparum</i> L.	UR	Polygonaceae perennial herb
LR	The lower reaches of the HRB	–	SC	<i>Stipa capillata</i> Linn	UR	Gramineous perennial herb
Qilian Mt.	Qilian Mountains of the UR	UR	SP	<i>Stipa purpurea</i> Griseb	UR	Gramineous perennial herb
QSF	Qinghai spruce forest	UR	BA	<i>Berberis amurensis</i>	UR	Deciduous shrubs or small trees
MG	Mountain grassland	UR	HA	<i>Haloxylon ammodendron</i>	MR and LR	Deciduous shrubs or small trees
MM	Mountain meadow	UR	TR	<i>Tamarix ramosissima</i> Ledeb	MR and LR	Ultraxerophytic shrubs
SM	Swamp meadow	UR	RS	<i>Reaumuria soongorica</i> Maxim	MR and LR	Perennial deciduous shrubs
DO	Desert–oasis ecotone	MR	NT	<i>Nitraria tangutorum</i> Bobr	MR	Deciduous shrubs
GB	Gobi	MR and LR	PE	<i>Populus euphratica</i> Oliv	LR	Deciduous broadleaf tree
RF	Riparian forest	LR	SA	<i>Sophora alopecuroides</i>	LR	Leguminous perennial herb

Table 2 The sampling species, sampling plant components, and sampling dates in different regions of the Heihe River Basin.

Study region	Ecosystem type	Study time	Locations	Altitude (m)	Longitude	Latitude	Dominated plant species	Groundwater level	
UR	Mountain grassland	7 June 2009	U1	2774	99.9	38.8	SC root and leaf		
	Swamp meadow	7 June 2009	U2	3040	99.9	38.8	PV root and leaf		
	Mountain meadow	8 June 2009	U3	3476	99.5	38.6	SP root and leaf		
	Swamp meadow	8 June 2009	U4	3732	99.6	38.6	SC root and leaf		
	Qinghai spruce forest	21 August 2007	U5	2594	100.3	38.6	QS, PF and BA stem and leaf		
		7 June 2009	U6	2654	99.6	38.8	QS stem and leaf		
		27–28 June 2011	U8-11	2780	100.3	38.6	QS stem and SC root and leaf		
		1 August 2012	U8-12				QS stem		
		23–25 June 2011	U9-6	2900	100.3	38.5	QS and PF stem and PV root and leaf		
2–8 September 2011	U9-9								
MR	Desert–oasis ecotone	15–16 June 2010	M1-10	1386	100.1	39.4	TR stem and leaf		
		3 August 2012	M1-12				TR stem		
		15–16 June 2010	M2-10	1386	100.1	39.4	HA stem and leaf		
		3 August 2012	M2-12				HA stem		
		4 August 2012	M3-12	1440	–	–	HA stem		
	Gobi	27 August 2007	M4-07	1413	100.1	39.4	RS stem and leaf		
		18–19 June 2010	M4-10				RS and NT stem and leaf		
		5 August 2012	M4-12				RS stem		
LR	Riparian forest	6–9 August 2009	L1-09	930	101.2	42.0	PE stem and SA root and leaf	1.8 m	
		21–22 June 2010	L1-10					2.0 m	
		8 August 2012	L1-12				PE stem	2.0 m	
		21–22 June 2010	L2-10	930	101.2	42.0	TR stem and leaf	2.0 m	
		8 August 2012	L2-12				TR stem	2.0 m	
	Planted shrubland	20 August 2012	L3-08	920	101.1	42.0	PE and TR stem and SA and leaf	> 10.0 m	
		20 August 2012	L4-08	921	101.1	42.0			
		23–24 June 2010	L5-10	910	101	41.9	HA stem and leaf	2.5 m	
		9 August 2012	L5-12				HA stem	2.2 m	
		Gobi	26–27 June 2010	L6-10	906	101.1	42.3	RS stem and leaf	> 5.0 m
			11 August 2012	L6-12				RS stem	

The UR, MR, and LR indicate the upper, middle, and lower reaches of the Heihe River Basin. The numbers after U, M, and L are site numbers. The SC, PV, SP, QS, PF, BA, PV, TR, HA, RS, PE and SA indicate *Stipa capillata* Linn, *Polygonum viviparum* L., *Stipa purpurea* Griseb, Qinghai Spruce, *Potentilla fruticosa* L., *Berberis amurensis*, *Polygonum viviparum* L., *Tamarix ramosissima* Ledeb, *Haloxylon ammodendron*, *Reaumuria soongorica* Maxim, *Populus euphratica* Oliv and *Sophora alopecuroides*, respectively.

mountain meadows, high mountain meadows, swamp meadows, and forests (Zhao *et al.*, 2020; Fig. S1). In the middle reaches, due to the absence of long-term climatic data in Linze (middle reaches), we used climatic data in Zhangye meteorological station (100°26'N, 38°56'E, elevation: 1483 m asl), which is about 60 km from Linze. The long-term mean annual precipitation is 130 mm, with 73.7% of the rainfall occurring between June and September. The main ecosystem types are planted oasis, desert–oasis ecotone, and Gobi Desert in the middle reaches of the Heihe River Basin (Fig. S1). In the lower reaches (Ejina: 101°04'N, 41°57'E, elevation: 941 m asl), the long-term (1960–2012) mean annual precipitation is 34 mm, with 74.3% of the rainfall occurring between June and September. The Ejina is considered one of the driest regions in China. The main ecosystem types in the lower reaches are riparian forest, planted shrubland, and the Gobi Desert (Zhao *et al.*, 2020; Fig. S1).

Field sampling

Between 2007 and 2012, several field campaigns were conducted during the growing seasons in the different regions. Deep and

shallow soil samples, plant roots (grasses), stems (trees and shrubs) and leaves were sampled in June 2009 and 2011, August 2007, 2009 and 2012 and September 2011 in the upper reaches, July and August 2007, June 2010 and August 2012 in the middle reaches, and June 2007 and 2010, August 2008, 2009 and August 2012 in the lower reaches of the Heihe River Basin. Precipitation samples were collected at Yeniugou (P1: 3320 m asl), Hulugou (P2: 3020 m asl) and Pailugou (P3: 2700 m asl) in the upper reaches, at Zhangye (P4: 1483 m asl) in the middle reaches and at Ejina (P5: 920 m asl) in the lower reaches (Fig. S1a). The stable isotope composition of previous years precipitation (1986–2003) at Zhangye was obtained from the GNIP database (<http://nds121.iaea.org/wiser>). Detailed sampling information is shown in Tables 1 and 2 and the Methods S1.

Water sample extraction

The extraction of water from the soil, stems, roots, and leaves was performed with a cryogenic vacuum distillation system (Zhao *et al.*, 2016, 2019, 2020), based on the design and methodology described by Ehleringer *et al.* (2000) and West *et al.* (2006).

Samples in extraction vials were heated to 100°C and evaporated water was trapped in U-tubes, submerged in liquid nitrogen. The pressure in the vacuum line was continuously recorded using sub-atmosphere pressure sensors (APG100; Active Pirani vacuum gages, Edwards, UK) to ensure it remained leak-tight throughout the extraction. The cryogenic vacuum distillation method is widely used for plant tissues and is considered a reliable standard against which other extraction methods can be compared. The fractionation during sample distillation does not have any significant effect on the isotopic composition of the water samples that are recovered if the distillation is taken to completion (Ellsworth & Williams, 2007), and when > 600 µl of water was extracted for samples at natural isotope abundance (Diao *et al.*, 2022). In our study, the extracted water amount of most samples was > 1000 µl. In addition, the $\delta^{18}\text{O}$ of mobile xylem water extracted from stem xylem tissues by mild vacuum extraction did not differ from that of immobile xylem water extracted later from the same tissues by cryogenic distillation (Cernusak *et al.*, 2005). West *et al.* (2006) estimated minimum extraction times to be 60–75 min for woody stems, 40 min for clay soils, 30 min for sandy soils, and 20–30 min for leaves during vacuum distillation to obtain an unfractionated water sample. In our study, extraction was performed under a vacuum of 0.03 hPa for at least 2 h in order to ensure an unfractionated water sample (West *et al.*, 2006). The resulting extracted water samples were then sealed with Parafilm, placed in a bath, and allowed to thaw. Lastly, the liquid water was transferred to a 2 ml vial for $\delta^{18}\text{O}$ and $\delta^2\text{H}$ analysis.

Stable isotope analysis

The $\delta^{18}\text{O}$ and $\delta^2\text{H}$ values of the water samples were measured using an Isoprime isotope ratio mass spectrometer (GV Instruments, Manchester, UK) coupled to a Euro EA3000 element analyzer at Heihe Key Laboratory of Ecohydrology and River Basin Science, Northwest Institute of Eco-Environment and Resources, Chinese Academy Sciences. To avoid any memory effect associated with continuous-flow methods, measurements of each sample were repeated five times, and the first values were discarded. The accuracy was better than $\pm 1.0\text{‰}$ for $\delta^2\text{H}$ and $\pm 0.2\text{‰}$ for $\delta^{18}\text{O}$. We first used three international standard materials: the Vienna Standard Mean Ocean Water (V-SMOW), Greenland Ice Sheet Precipitation (GISP), and Standard Light Antarctic Precipitation (SLAP) to calibrate our working standards. We selected one (or two) international standard and two (or one) of the three lab working standards for calibration purposes according to the sample delta ranges (Zhao *et al.*, 2016, 2019). For example, we used V-SMOW, BJD, and LZPW to calibrate soil water data, used V-SMOW, LZPW, and LZI to calibrate plant water data and used SLAP, BJD, and LZI to calibrate precipitation, respectively. The $\delta^{18}\text{O}$ and $\delta^2\text{H}$ values are expressed in ‰ on a V-SMOW–SLAP scale.

Measurements of $\delta^{18}\text{O}$ and $\delta^2\text{H}$ composition of xylem water (δ_{Xylem}), leaf water (δ_{Leaf}), and potential water source (δ_{Soil} and/or $\delta_{\text{Groundwater}}$) were performed for dominant trees, shrubs, and grasses growing in the natural habitat from upper, middle

and lower reaches of the Heihe River Basin. To avoid the potential bias resulting from organics in δ_{Xylem} , δ_{Leaf} and δ_{Soil} , the $\delta^2\text{H}$ and $\delta^{18}\text{O}$ of soil water, xylem water, leaf water samples, and precipitation samples collected before 2010 were all determined using the EA + IRMS system (Zhao *et al.*, 2011). This method is a mass-based analysis, and trace amounts of contaminants are unlikely to have a large effect on the isotopic value of a water sample measured by IRMS (West *et al.*, 2010). Precipitation samples since 2010 were measured using an L1102-I isotopic water analyzer (Picarro, Sunnyvale, CA, USA).

Theoretical considerations/background

To assess the hydrogen isotopic offset between plant xylem water and its potential sources, Landwehr & Coplen (2004) proposed the concept of the line-conditioned excess (LC-excess = $\delta^2\text{H} - a \times \delta^{18}\text{O} - b$, where a and b correspond to the slope and intercept of the LMWL, respectively). Because the source water for plants is more likely soil water or/and groundwater than rain-water directly, Barbata *et al.* (2019) and Li *et al.* (2021) modified the equation above and computed the deviation of a given xylem water with respect to the soil water evaporated line (SW-excess = $-\delta^2\text{H} - a_s \times \delta^{18}\text{O} - b_s$; where a_s and b_s are the slope and intercept of the soil water evaporated line for a given plot and date, respectively, and $\delta^2\text{H}$ and $\delta^{18}\text{O}$ correspond to the isotopic composition of a xylem water sample collected on that plot at that date) (Barbata *et al.*, 2019) and a potential water source line (PWL-excess = $\delta^2\text{H} - a_{\text{pw}} \times \delta^{18}\text{O} - b_{\text{pw}}$; a_{pw} linear regression line between $\delta^{18}\text{O}$ and $\delta^2\text{H}$ data of both soil water and groundwater. a_{pw} and b_{pw} are the slope and intercept of the soil water and groundwater line for a given site and date, respectively) (Li *et al.*, 2021) to correct $\delta^2\text{H}$ offsets of stem water. The SW-excess/PWL-excess of xylem water are indicators of the $\delta^2\text{H}$ offsets between xylem water and their corresponding soil water evaporated line/potential water source line. We calculated the hydrogen isotopic offset as LC-excess (Landwehr & Coplen, 2004), SW-excess (Barbata *et al.*, 2019), and PWL-excess (Li *et al.*, 2021) by comparing the stable isotopic composition of xylem waters with the potential water sources of plants assuming no oxygen isotope fractionation during plant water uptake. Negative $\delta^2\text{H}$ offsets indicate that $\delta^2\text{H}$ of xylem water are more depleted than $\delta^2\text{H}$ of their potential water sources such as soil water or both soil water and groundwater (plots of $\delta^{18}\text{O}/\delta^2\text{H}_{\text{Xylem}}$ are thus positioned below the plots of $\delta^{18}\text{O}/\delta^2\text{H}$ of their potential water sources in a $\delta^{18}\text{O}$ – $\delta^2\text{H}$ diagram; Figs 1, S2Aa–c, Ba, b, d, f, Ca–d, De, f; Barbata *et al.*, 2019; Li *et al.*, 2021). Near-zero $\delta^2\text{H}$ offsets indicate xylem water samples that are neither enriched nor depleted in deuterium compared to $\delta^2\text{H}$ of their potential water sources. Therefore, plots of $\delta^{18}\text{O}/\delta^2\text{H}_{\text{Xylem}}$ are positioned close to the plots of $\delta^{18}\text{O}/\delta^2\text{H}$ of their potential water sources in a $\delta^{18}\text{O}$ – $\delta^2\text{H}$ diagram if there is no ^{18}O fractionation (Figs 1, S2Bf, Dg, h). However, positive $\delta^2\text{H}$ offsets indicate xylem water samples that are more enriched in deuterium compared to the $\delta^2\text{H}$ of their potential water sources. This is reflected by the position of plots of $\delta^{18}\text{O}/\delta^2\text{H}_{\text{Xylem}}$ being above the plots of $\delta^{18}\text{O}/\delta^2\text{H}$ of their water sources in a $\delta^{18}\text{O}$ – $\delta^2\text{H}$ diagram (Figs 1, S2Ad, Bc). In our study,

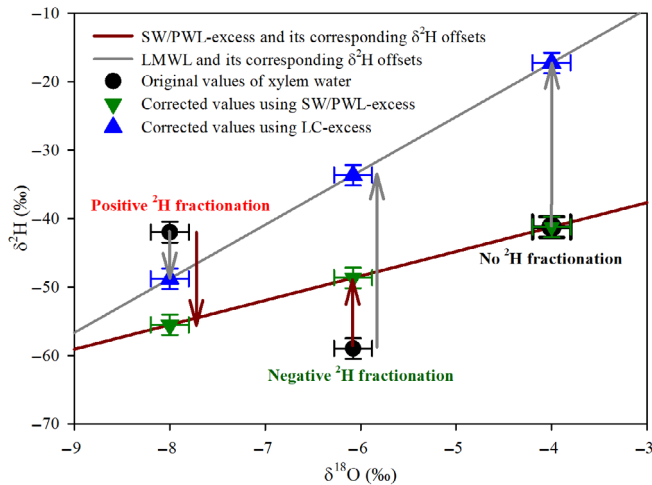


Fig. 1 A conceptual graph of the potential water line in the $\delta^2\text{H}/\delta^{18}\text{O}$ space against plant xylem water, locations of $\delta^2\text{H}/\delta^{18}\text{O}_{\text{xylem}}$ water under positive, negative, and no ^2H fractionations and the $\delta^2\text{H}$ offsets corrected by both SW/PWL-excess (dark red arrows) and LC-excess methods (gray arrows).

we utilized the SW-excess when assuming plants only use soil water sources (Barbeta *et al.*, 2019), while we employed the PWL-excess when assuming plants use both soil water and groundwater due to there being differences between $\delta_{\text{soil water}}$ and $\delta_{\text{groundwater}}$ (Zhao *et al.*, 2020; Li *et al.*, 2021).

Data analyses

Statistical significance of the $\delta^2\text{H}$ offset was tested compared to zero with software SPSS (version 22). All statistical analyses were performed with R software (R Core Team, 2022). Before constructing models including General Linear Mix-effects Models (GLMMs) or Linear Mixed Model (LMMs), we used the variance inflation factor (VIF) to diagnose the collinearity of explanatory variables (e.g. high correlation among explanatory variables). Furthermore, we built Structural Equation Models (SEMs) to evaluate the direct and indirect factors contributing to the standardized total effect. The cause correlations among variables were determined based on our known ecophysiological knowledge. SEM was performed using the lavaan package in R (Rosseel, 2012). In SEM analyses, data were fitted to the model using the likelihood estimation method. The adequacy of the model was determined using the comparative-of-fit (cif) index, the root mean squared error of approximation (rmsea) and the standardized root mean square residual (srmr). Favorable models showed higher gif (>0.9), lower rmsea (<0.08), and srmr (<0.08) values in the SEM results.

Results

The plant water source $\delta^2\text{H}$ offset along the Heihe River Basin

Along the strong climate gradient of the Heihe River basin, among 635 measurements from 43 field observations, 29 of 43

observations (*c.* 67%) exhibited negative $\delta^2\text{H}$ offset, 4 of 43 (*c.* 9%) observations showed positive $\delta^2\text{H}$ offset, and 10 of 43 observations (*c.* 23%) exhibited nonsignificant $\delta^2\text{H}$ offset on the basin scale (Table 3). In the upper reaches (cold and moist environment, Fig. S1), among 285 measurements from 10 sites with 17 field observations, 11 of 17 observations (*c.* 65%) exhibited negative $\delta^2\text{H}$ offset, 3 of 17 (*c.* 18%) observations showed positive $\delta^2\text{H}$ offset, and 3 of 17 observations (*c.* 18%) exhibited nonsignificant $\delta^2\text{H}$ offset (Table 3). The mean $\delta^2\text{H}$ offsets were -3.6‰ and varied from -12.5 ± 1.8 ($n=3$) (*Stipa capillata* Linn (SC) in U1) to $4.8\text{‰} \pm 4.7$ ($n=26$) (*Polygonum viviparum* L. (PV) in U9-9). For the middle reaches (transitional zone, Fig. S1) with 98 measurements from 9 sites, *c.* 44% (4 of 9) of the cases show remarkable negative $\delta^2\text{H}$ offsets, and *c.* 11% (1 of 9) of the cases show remarkable positive $\delta^2\text{H}$ offsets (Table 3). The mean $\delta^2\text{H}$ offsets were -1.5‰ and varied from -7.1 ± 2.6 ($n=14$) (*Tamarix ramosissima* Ledeb (TR) in M1-12) to $4.1\text{‰} \pm 1.8$ ($n=3$) (*Reaumuria soongorica* Maxim (RS) in M4-07 with nonsignificant) (Table 3). However, in warm-dry lower reaches with 232 measurements, 14 of 17 observations (*c.* 82%) exhibited negative $\delta^2\text{H}$ offset, and 3 of 17 observations (*c.* 18%) exhibited nonsignificant $\delta^2\text{H}$ offset (Table 3). The mean $\delta^2\text{H}$ offsets were -5.1‰ , and varied from -9.5 ± 1.5 ($n=13$) (TR in L4-08) to $1.0\text{‰} \pm 1.3$ ($n=14$) (RS in L6-10 with nonsignificant). However, there were no consistent change patterns in $\delta^2\text{H}$ offsets for different plant species (Fig. 2).

Effects of climate on plant water source $\delta^2\text{H}$ offsets

The complex correlations between $\delta^2\text{H}$ offsets and climate at different spatial and plant functional type scales were revealed (Figs 3a,b, 4a,b, S3a,b, S4a,b, S5a,b, S6a,b). Across the entire basin, significantly negative relationships between $\delta^2\text{H}$ offset and temperature ($R^2=0.23$, $P<0.001$, $n=635$) and significantly positive relationships between $\delta^2\text{H}$ offset and relative humidity ($R^2=0.11$, $P<0.001$, $n=635$) were found. At the reach scale, significantly negative relationships between $\delta^2\text{H}$ offsets and temperature were found in the upper reaches and middle reaches, and the slopes decreased sharply from the upper ($-0.528\text{‰}/\text{°C}$), middle ($-0.262\text{‰}/\text{°C}$) to lower reaches ($-0.064\text{‰}/\text{°C}$; Fig. 4a). Significantly positive relationships between $\delta^2\text{H}$ offsets and relative humidity were only revealed in the upper reaches (Fig. 4b).

We classified all plant species into trees, shrubs, and grasses to reveal the plant functional type response of $\delta^2\text{H}$ offset to both temperature and relative humidity (Figs 3a,b, S4a,b, S5a,b). There were significantly negative relationships between $\delta^2\text{H}$ offsets and temperature, and significantly positive relationships between $\delta^2\text{H}$ offsets and relative humidity. In addition, the response patterns of $\delta^2\text{H}$ offsets to both temperature (negative) and relative humidity (positive) were similar in explained variances and slopes at the basin scale (Fig. 3a). However, at the reach scale, in the upper reaches, there were significantly negative relationships between the trees, shrubs and grasses $\delta^2\text{H}$ offsets and temperature, and the slopes were $-0.701\text{‰}/\text{°C}$ in grasses, $-0.672\text{‰}/\text{°C}$ in shrubs and $-0.380\text{‰}/\text{°C}$ in trees (Fig. S7a). Significantly positive relationships between the $\delta^2\text{H}$ offset and

Table 3 The plant water source $\delta^2\text{H}$ offset occurred between plant potential water sources and xylem water, oxygen and hydrogen isotopic compositions of xylem water ($\delta^{18}\text{O}_{\text{Xylem}}$, $\delta^2\text{H}_{\text{Xylem}}$), of leaf water ($\delta^{18}\text{O}_{\text{Leaf}}$) and difference of $\delta^{18}\text{O}_{\text{Leaf}}$ and $\delta^2\text{H}_{\text{Xylem}}$ ($\Delta^{18}\text{O}_{\text{Leaf-Xylem}}$) in the various plants along the climate gradient from cool-moist to warm-arid environments across the inland Heihe River Basin, northwestern China.

Region	ID	Plant species	Methods	$\delta^2\text{H}$ offsets	SD	$\delta^{18}\text{O}_{\text{Xylem}}$	SD	$\delta^2\text{H}_{\text{Xylem}}$	SD	$\delta^{18}\text{O}_{\text{Leaf}}$	SD	$\Delta^{18}\text{O}_{\text{Leaf-Xylem}}$	SD
The UR	U1	SC	SW-excess	-12.5** (3)	1.8	-3.0	0.3	-50.3	2.4	10.7	0.6	13.7	0.6
	U2	PV	SW-excess	-10.3** (3)	1.3	-6.1	0.5	-59	2.9	7.3	1.1	13.4	0.9
	U3	SP	SW-excess	-6.6** (3)	1.0	-1.4	0.5	-38.5	2.5	18.9	2.0	20.3	1.7
	U4	SC	SW-excess	-8.4* (3)	2.5	-3.5	0.3	-47.8	1.8	11.0	1.0	14.4	0.8
	U5	QS	SW-excess	3.0 ns (3)	1.4	-5.3	0.4	-37.3	2.7	11.8	1.3	17.0	1.4
		PF	SW-excess	0.5 ns (3)	0.6	-4.2	0.4	-36.2	1.9	9.8	1.6	14.1	1.9
		BA	SW-excess	1.6 ns (3)	0.7	-4.9	0.3	-37.4	1.8	14.0	1.0	18.9	2.4
	U6	QS	SW-excess	-9.2** (3)	0.6	-6.4	0.5	-53.5	2.3	21.0	1.2	27.4	1.7
	U8-11	QS	SW-excess	-3.0*** (37)	2.0	-5.9	0.7	-45.6	3.6	16.0	1.7	21.9	1.5
		SC	SW-excess	-4.9*** (19)	3.5	-1.7	1.6	-32.7	7.3	8.2	2.5	10.0	2.5
	U8-12	QS	SW-excess	-11.2*** (8)	3.8	-7.3	2.0	-58.8	5.5	nd	nd	nd	nd
	U9-6	QS	SW-excess	-5.7*** (42)	1.9	-7.8	0.7	-57.8	4.3	7.3	5.8	15.1	5.7
		PF	SW-excess	-3.1*** (22)	3.0	-5.7	1.0	-46.1	6.2	1.6	5.2	7.3	5.9
		PV	SW-excess	-1.6*** (21)	1.7	-6.9	0.8	-49.6	3.9	0.9	5.4	7.7	5.1
	U9-9	QS	SW-excess	1.9*** (60)	1.4	-7.6	0.4	-49.0	2.7	4.3	5.7	11.7	5.5
		PF	SW-excess	4.2*** (26)	3.8	-4.4	0.7	-33.2	5.8	4.2	7.2	8.6	7.3
		PV	SW-excess	4.8*** (26)	4.7	-6.2	1.1	-40.5	7.0	2.0	8.2	8.2	7.9
	The MR	M1-10	TR	PWL-excess	-2.1*** (14)	1.8	-7.3	0.6	-58.0	1.7	10.6	7.2	18.0
M1-12		TR	PWL-excess	-7.1*** (14)	2.6	-7.7	0.4	-63.2	2.8	nd	nd	nd	nd
M2-10		HA	SW-excess	3.6*** (14)	1.8	0.1	1.5	-29.9	5.6	19.0	4.4	18.9	4.5
M2-12		HA	SW-excess	-6.6* (4)	2.7	0.7	0.7	-39.6	5.4	nd	nd	nd	nd
M3-12		HA	PWL-excess	-5.9*** (5)	1.4	-7.6	1.6	-70.5	4.6	nd	nd	nd	nd
M4-07		RS	SW-excess	4.1 ns (3)	1.8	-3.5	0.4	-47.4	2.9	15.0	0.9	18.6	0.6
M4-10		RS	SW-excess	1.8 ns (13)	2.6	0.1	0.9	-34.5	5.2	32.7	3.8	32.6	3.9
		NT	SW-excess	0.4 ns (13)	3.3	0.3	1.4	-35	7.0	32.4	3.0	32.1	2.9
M4-12		RS	SW-excess	-1.8 ns (18)	3.1	1.9	0.7	-30.8	4.4	nd	nd	nd	nd
The LR		L1-09	PE	PWL-excess	-6.3*** (36)	0.9	-5.3	0.3	-49.4	1.0	14.6	5.0	19.7
		SA	PWL-excess	-6.7** (6)	3.7	-2.6	0.5	-45.7	4.4	16.6	3.0	19.1	3.0
	L1-10	PE	PWL-excess	-5.3*** (13)	1.4	-6.2	0.4	-50.1	1.7	16.8	3.1	23.0	3.1
		SA	PWL-excess	-3.8*** (10)	0.9	-5.3	0.5	-47	1.0	16	3.7	20.0	4.5
	L1-12	PE	PWL-excess	-4.7*** (29)	2.8	-4.8	0.6	-47.1	3.4	nd	nd	nd	nd
	L2-10	TR	PWL-excess	-6.4*** (13)	1.4	-5.0	0.7	-49.2	1.4	14.9	5.6	19.9	6.0
	L2-12	TR	PWL-excess	-7.9*** (17)	2.9	-5.6	1.2	-51.7	4.0	nd	nd	nd	nd
	L3-08	PE	PWL-excess	-2.7*** (18)	1.2	-7.8	0.4	-58.7	1.4	15.6	3.6	23.4	3.7
		TR	PWL-excess	-7.0*** (18)	1.7	-6.5	0.4	-60.2	2.3	14.3	3.6	20.8	3.7
		SA	PWL-excess	-4.6*** (18)	2.1	-5.6	1.0	-55.9	4.1	18.7	2.1	24.3	2.0
	L4-08	PE	PWL-excess	-0.6 ns (9)	0.8	-6.9	0.1	-50.1	0.9	16.4	3.3	23.3	3.3
		TR	PWL-excess	-9.5*** (9)	2.4	-5.4	0.2	-55.1	2.5	15.6	6.2	21	6.1
		SA	PWL-excess	-3.9** (9)	2.6	-3.8	0.9	-45.3	4.4	17.5	3.5	21.3	3.3
	L5-10	HA	PWL-excess	-9.5*** (13)	1.5	-7.2	0.4	-71.0	1.7	15.8	2.7	23.1	2.9
	L5-12	HA	PWL-excess	-7.6*** (23)	3.4	-7	1.3	-66.8	6.2	nd	nd	nd	nd
	L6-10	RS	SW-excess	1.0 ns (14)	1.3	-3.1	0.8	-51.6	2.9	12.8	8.9	15.8	8.9
L6-12	RS	SW-excess	-1.2 ns (6)	3.4	-2.2	0.8	-54.3	3.8	nd	nd	nd	nd	

The UR, MR, and LR indicate the upper, middle, and lower reaches of the Heihe River Basin. The numbers after U, M, and L are site numbers. The plant function types were indicated with different colors (grass – blue; shrub – green; tree – brown). The presence of an asterisk indicates that the value is significantly different from zero (*, $P < 0.05$; **, $P < 0.01$; ***, $P < 0.001$; ns, not significant), the number in the brackets indicates the sample number. The SC, PV, SP, and SA indicate grasses *Stipa capillata* Linn, *Polygonum viviparum* L., *Stipa purpurea* Griseb, and *Sophora alopecuroides*, respectively. PF, BA, RS, TR, HA, and NT indicate shrubs *Potentilla fruticosa* L., *Berberis amurensis*, *Reaumuria soongorica* Maxim, *Tamarix ramosissima* Ledeb, *Haloxylon ammodendron*, and *Nitraria tangutorum* Bobr, respectively. QS and PE indicate trees Qinghai Spruce and *Populus euphratica* Oliv, respectively. nd, no data.

relative humidity were also found, and the slopes were 0.149‰/‰ in grasses, 0.132‰/‰ in shrubs, and 0.087‰/‰ in trees (Fig. S7b). In the middle reaches, only a weak negative significant relationship between the $\delta^2\text{H}$ offsets and temperature (Figs 4a,b, S6a,b), and a weak positive relationship between the $\delta^2\text{H}$ offsets and relative humidity ($P < 0.05$; Figs S5a,b, S6a,b) were found for shrubs (Figs 4a,b, S6a,b).

Responses of plant water source $\delta^2\text{H}$ offsets to $\delta^{18}\text{O}$ of plant leaf water

There were significantly negative correlations of $\delta^2\text{H}$ offsets with both $\delta^{18}\text{O}_{\text{leaf}}$ (-0.099‰/‰) and $\Delta^{18}\text{O}_{\text{Leaf-xylem}}$ (-0.148‰/‰) based on 511 data pairs at the basin scale (Figs S3c,d, S6c,d). Significantly negative relationships between the $\delta^2\text{H}$ offsets with

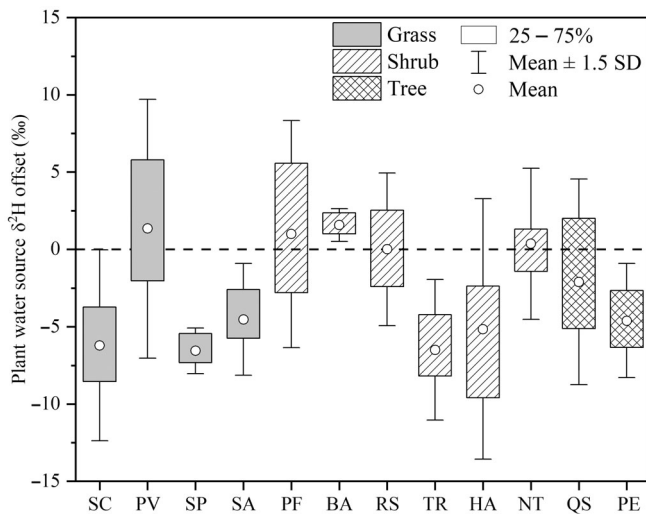


Fig. 2 Box-plot of species-specific plant water source $\delta^2\text{H}$ offset of different plant functional types in the Heihe River Basin. The SC, PV, SP, and SA indicate grasses *Stipa capillata* Linn, *Polygonum viviparum* L., *Stipa purpurea* Griseb, and *Sophora alopecuroides*, respectively. PF, BA, RS, TR, HA, and NT indicate shrubs *Potentilla fruticosa* L., *Berberis amurensis*, *Reaumuria soongorica* Maxim, *Tamarix ramosissima* Ledeb, *Haloxylon ammodendron* and *Nitraria tangutorum* Bobr, respectively. QS and PE indicate trees Qinghai Spruce and *Populus euphratica* Oliv, respectively. The error bars represent 1 SD.

$\delta^{18}\text{O}_{\text{leaf}}$ (-0.197‰) and $\Delta^{18}\text{O}_{\text{leaf-xylem}}$ (-0.195‰) were also found in the upper reaches (Figs 4c,d, S6c,d). However, weak significantly positive correlations of the $\delta^2\text{H}$ offsets with $\delta^{18}\text{O}_{\text{leaf}}$ (-0.130‰) and $\Delta^{18}\text{O}_{\text{leaf-xylem}}$ (-0.101‰) were found in the lower reaches (Figs 4c,d, S6c,d).

Regarding different plant functional types, the correlations between $\delta^2\text{H}$ offset with $\delta^{18}\text{O}_{\text{leaf}}$ and $\Delta^{18}\text{O}_{\text{leaf-xylem}}$ of trees and grasses were significantly negative, while shrubs were weak with $\Delta^{18}\text{O}_{\text{leaf-xylem}}$ and not significant with $\delta^{18}\text{O}_{\text{leaf}}$ at the basin scale (Fig. 3c,d). At the reach scale, trees (-0.171‰) and grasses (-0.274‰) showed significant negative correlations with $\delta^{18}\text{O}_{\text{leaf}}$ and trees with $\Delta^{18}\text{O}_{\text{leaf-xylem}}$ (-0.207‰) with low explained variance in the upper reaches (Figs S4c,d, S6c,d). In the lower reaches, $\delta^2\text{H}$ offsets of shrubs had significantly positive correlations with $\delta^{18}\text{O}_{\text{leaf}}$ (0.206‰ , $P=0.033$), and $\delta^2\text{H}$ offsets of trees had significantly positive correlations with $\Delta^{18}\text{O}_{\text{leaf-xylem}}$ (0.121‰ , $P=0.038$) (Figs S5c,d, S6c,d).

Discussion

The plant water source $\delta^2\text{H}$ offset

The isotopic composition of stem water sometimes does not match any of the considered sources in the dual-isotope space and xylem water samples plot well below the soil water line in the $\delta^{18}\text{O}$ – $\delta^2\text{H}$ space (Renée Brooks *et al.*, 2009; Evaristo *et al.*, 2017; Geris *et al.*, 2017; Vargas *et al.*, 2017; Wang *et al.*, 2017; Deurwaerder *et al.*, 2018; Oerter & Bowen, 2019). This suggested that hydrogen isotope fractionation may occur

during root water uptake, or water transport/redistribution within the plants (Lin & Sternberg, 1992; Ellsworth & Williams, 2007; Zhao *et al.*, 2016; Evaristo *et al.*, 2017; Geris *et al.*, 2017; Newberry *et al.*, 2017; Vargas *et al.*, 2017; Wang *et al.*, 2017; Deurwaerder *et al.*, 2018; Barbeta *et al.*, 2019, 2020; Oerter & Bowen, 2019). Instead, xylem water samples plotting close to the soil water line in the $\delta^{18}\text{O}$ – $\delta^2\text{H}$ space could indicate the absence of fractionation during root water uptake, but could also indicate the existence of opposed processes (e.g. depletion compensated by evaporative enrichment). The xylem water $\delta^{18}\text{O}$ – $\delta^2\text{H}$ space below/above/on their potential water source line (SW-excess/PWL-excess) in our study (Fig. S2) suggested negative/positive/no fractionation in deuterium occurring during root water uptake or water transport/redistribution in the inland Heihe River Basin. We then used the plant water source $\delta^2\text{H}$ offset (the $\delta^2\text{H}$ offset) to reveal ^2H fractionation direction and strength (Barbeta *et al.*, 2019; Li *et al.*, 2021). We found different $\delta^2\text{H}$ offset patterns among geographical environments and that ^2H fractionation was a common phenomenon, with negative/positive/no fractionation (Table 3). A previous study (Casa *et al.*, 2022) reported that the deviation in the isotopic composition of stem water from soil water varied substantially in size and direction, but, on average, it was slightly more negative than soil water. However, our results revealed that $\delta^2\text{H}$ offset could be negative, zero, and positive (Table 3). In the upper reaches (cold and moist environment, Fig. S1), we found several interesting phenomena: (1) significantly negative $\delta^2\text{H}$ offset occurred during the strong growth period from June to early August (Tables 2 and 3), suggesting that when temperature is the limiting factor, the more active plant growth, the stronger transpirational water loss (Vargas *et al.*, 2017; Barbeta *et al.*, 2020), the stronger ^2H fractionation; (2) significantly positive $\delta^2\text{H}$ offset occurred during minimum plant physiological activity with low temperature (night temperature was below 4°C) during September, indicating that positive fractionation occurs when plant physiological activity is at the minimum; (3) non- $\delta^2\text{H}$ offset was found during the period with weak physiological activity at the end of August, implying that when plant physiological activity is low, fractionation does not occur such as QS, PF and PV in the upper reaches; (4) the zero, positive and negative $\delta^2\text{H}$ offsets occurred in the same species during their different growth periods such as PF in the upper reaches, and no ^2H fractionation occurred in the same species growing in different climatic conditions such as RS in the middle reaches and lower reaches (Table 3). This was different from the finding that $\delta^2\text{H}$ offset was more negative in cold and wet sites, whereas it was more positive in warm sites (Casa *et al.*, 2022). However, our results are consistent with the report of Barbeta *et al.* (2020) that regardless of substrate, soil, and stem water $\delta^2\text{H}$ were similar only near the permanent wilting point. Under moist conditions, stem water $\delta^2\text{H}$ was $11 \pm 3\text{‰}$ more negative than soil water $\delta^2\text{H}$, and under drier conditions, stem water $\delta^2\text{H}$ became progressively more enriched than soil water $\delta^2\text{H}$ in the temperate tree species *Fagus sylvatica* (Barbeta *et al.*, 2020), which supported our three cases. For the middle reaches, c. 44% of the cases show remarkable negative $\delta^2\text{H}$ offsets (Table 3), suggesting in this mountain front transitional zone

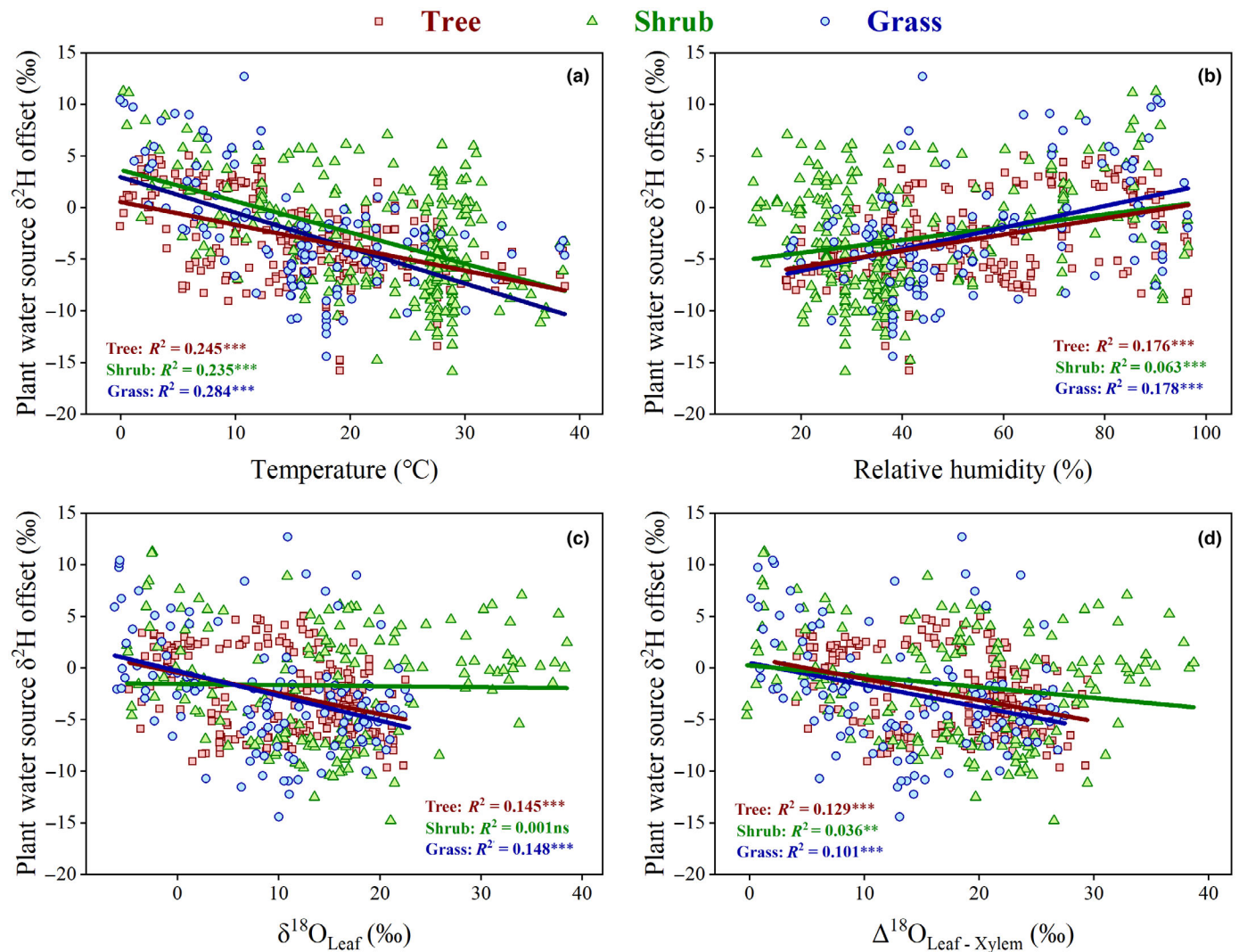


Fig. 3 The correlations between the $\delta^2\text{H}$ offsets and temperature (a), relative humidity (b), $\delta^{18}\text{O}_{\text{Leaf}}$ (c), and $\Delta^{18}\text{O}_{\text{Leaf-Xylem}}$ (d) based on the plant functional types (FTP). The FTPs across the Heihe River Basin are classified into grasses, shrubs, and trees with differing colors and shapes. *, $P < 0.05$; **, $P < 0.01$; ***, $P < 0.001$; ns, not significant.

with a mild environment, climate imposed some impacts on the occurrence of plant $\delta^2\text{H}$ offsets. However, in warm-dry lower reaches, c. 82% exhibited negative $\delta^2\text{H}$ offset, and we did not find significantly positive $\delta^2\text{H}$ offsets (Table 3), implying the potential strong influence of climates on the $\delta^2\text{H}$ offset. In addition, the discovery of negative, zero, and positive $\delta^2\text{H}$ offsets (Table 3) is against the viewpoint from Chen *et al.* (2020) that ^2H depletion is a common phenomenon, and is not necessarily restricted to a particular habitat type. Also, the existence of zero and positive $\delta^2\text{H}$ offsets in multiple cases suggests that negative offset is not necessarily all caused by cryogenic extraction (Chen *et al.*, 2020).

Species-specific variation in plant water source $\delta^2\text{H}$ offset

In the present study, we sampled 12 plant species in total, including six plant species in the upper reaches, four plant species in the

middle reaches, and five plant species in the lower reaches (Tables 2 and 3). In the upper reaches, for the tree *Qinghai Spruce* (QS), shrub *Potentilla fruticosa* L. (PF), and grass *Polygonum viviparum* L. (PV), there are positive/zero/negative $\delta^2\text{H}$ offset occurrences among the sites. These results revealed the varied ranges in $\delta^2\text{H}$ offsets of QS, PF, and PV depend on climate rather than plant species under cold and wet conditions. However, for the grasses *Stipa capillata* Linn (SC) and *Stipa purpurea* Griseb (SP), only negative $\delta^2\text{H}$ offsets occurred (Table 3). In the middle reaches, *Tamarix ramosissima* Ledeb (TR) exhibited a significantly negative $\delta^2\text{H}$ offset, and *Reaumuria soongorica* Maxim (RS) exhibited a nonsignificant $\delta^2\text{H}$ offset, while *Haloxylon ammodendron* (HA) exhibited both significantly negative and positive $\delta^2\text{H}$ offset (Table 3). For the lower reaches, excluding the RS with no ^2H fractionation, all other plant species showed significantly negative $\delta^2\text{H}$ offset (Table 3). From our results, the $\delta^2\text{H}$ offsets of QS, PF, and PV in the upper reaches were positive,

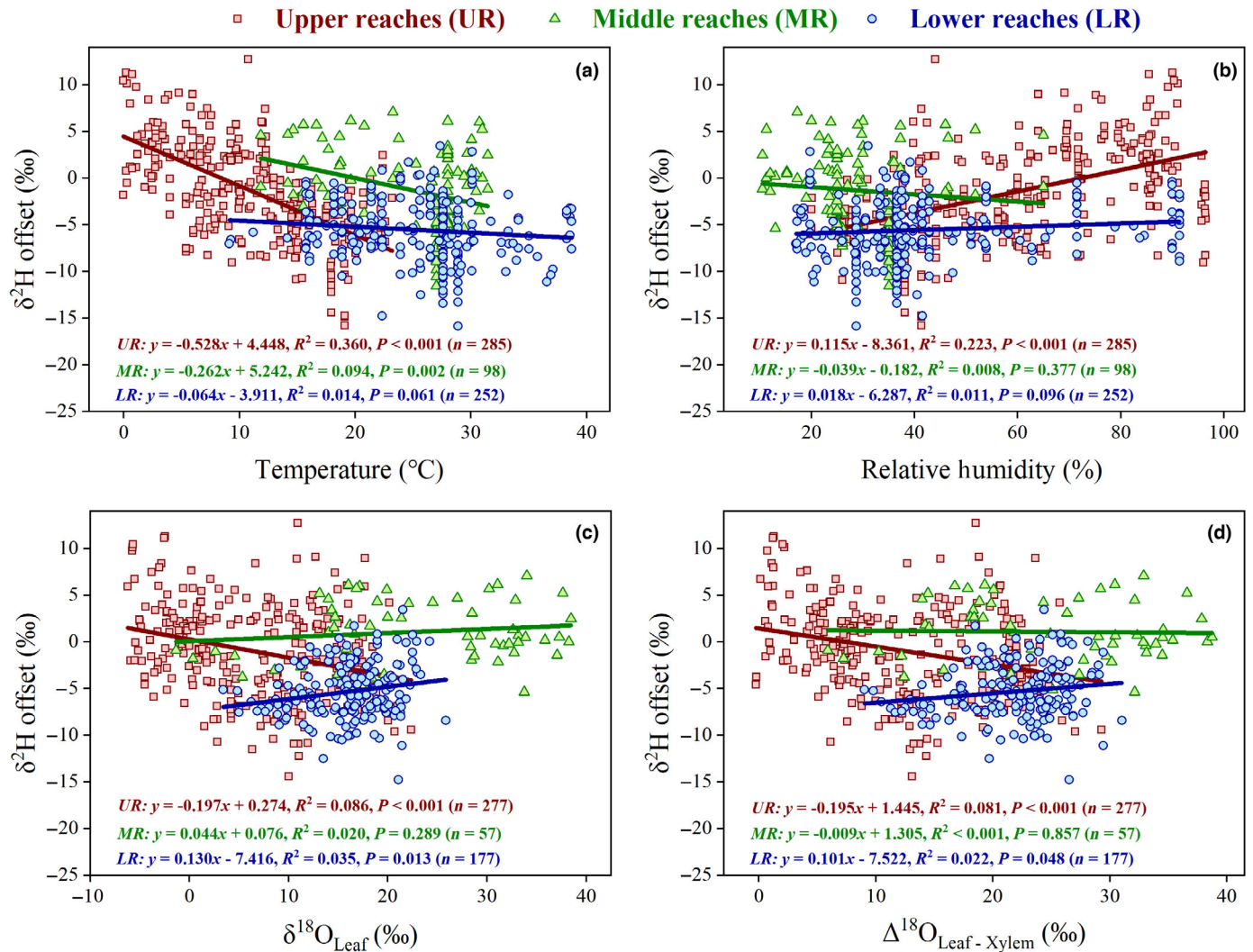


Fig. 4 Influences of temperature (a), relative humidity (b), $\delta^{18}\text{O}_{\text{Leaf}}$ (c), and $\Delta^{18}\text{O}_{\text{Leaf-xylem}}$ (d) on $\delta^2\text{H}$ offset of plants growing in the upper, middle, and lower reaches. The upper, middle, and lower reaches are shown with differing colors and shapes. The R^2 describes the goodness of the linear model. The regression functions and sample numbers are also shown. *, $P < 0.05$; **, $P < 0.01$; ***, $P < 0.001$; ns, not significant.

zero, and negative; the $\delta^2\text{H}$ offsets of HA in the middle were positive and negative, and in the lower reaches were negative, suggesting the $\delta^2\text{H}$ offsets were affected by climatic factors. However, the $\delta^2\text{H}$ offsets of SC in the upper reaches and of TR in the middle and lower reaches were negative, and of RS in the middle and lower reaches were near zero, which may be dependent on the plant species (Table 3). Our results reveal that varied ranges in $\delta^2\text{H}$ offsets depend on both plant species and climate, but with no clear plant functional type dependence (Fig. 2). For the trees, QS exhibited a large range but less $\delta^2\text{H}$ offset compared to *Populus euphratica* (PE), which may relate to difference in their eco-physiological characteristics (evergreen-needle vs deciduous broadleaf trees) and growth environment in the upper reaches and the lower reaches, respectively. For the six shrubs investigated, TR showed the strongest $\delta^2\text{H}$ offsets, followed by HA, while RS showed no ^2H fractionation. For the other three shrubs, slight positive $\delta^2\text{H}$ offsets were revealed. For four grass species,

except PV, 75% of species exhibit obviously negative $\delta^2\text{H}$ offsets (Fig. 2).

Effects of climate on plant water source $\delta^2\text{H}$ offset at different spatial scales

Pairwise regression analyses between the $\delta^2\text{H}$ offset and climate (temperature and relative humidity) across the plant functional types support strong and coherent effects related to climates (Figs 3a,b, 4a,b, S3a,b, S4a,b, S5a,b, S6a,b).

At the entire basin scale, compared to the positive relationships between $\delta^2\text{H}$ offset and relative humidity ($R^2 = 0.11$, $P < 0.001$, $n = 635$), stronger significantly negative relationships between $\delta^2\text{H}$ offset and temperature ($R^2 = 0.23$, $P < 0.001$, $n = 635$; Fig. S3a,b) revealed that the effects of temperature are much stronger on ^2H fractionation compared to that of relative humidity. This indicated the stronger contribution

in temperature-dependent ecophysiological and biochemical processes in ^2H fractionation than that from stomatal regulation related to air humidity. Our results contrasted with the positive relationship between $\delta^2\text{H}$ offset and temperature with extremely low explained variances at a global scale (Casa *et al.*, 2022). In addition, the climatic effects on $\delta^2\text{H}$ offset also suggest that methodological artifacts are unlikely to be the sole cause of observed isotopic offset (Casa *et al.*, 2022).

At the reach scale, significantly negative relationships between $\delta^2\text{H}$ offsets and temperature in the upper and middle reaches with a sharp decrease of the slopes from the upper to lower reaches were observed (Fig. 4a). By contrast, only significantly positive relationships between $\delta^2\text{H}$ offsets and relative humidity (0.115‰/%) in the upper reaches (Fig. 4b) revealed the reduced dependence of the $\delta^2\text{H}$ offset on temperature and relative humidity from the upper to lower reaches. In addition, we found a significantly negative exponent correlation ($R^2 = 0.67$, $P < 0.001$) between temperature and relative humidity (Fig. S7), suggesting some nonlinear superimposed effects of these two parameters on $\delta^2\text{H}$ offsets.

Regarding plant functional types, for temperature, differences in $\delta^2\text{H}$ offset dependence on temperature among plant functional types were minor with similar slopes and explained variance from the upper to lower reaches (Fig. 3a), which were consistent with the previous report (Casa *et al.*, 2022) that the $\delta^2\text{H}$ offset did not differ between angiosperms and gymnosperms, nor among growth forms (trees, shrubs and nonwoody plants), leaf habit (deciduous, evergreen, or semi-deciduous) or leaf shape (broad or narrow). For relative humidity, there was a relatively weak connection with $\delta^2\text{H}$ offset ($R^2 = 0.063$ *c.* 0.178, Fig. 3b). However, the substantial linkages between temperature (negative)/relative humidity (positive) and $\delta^2\text{H}$ offset are coherent and confirmed among plant functional types (Fig. S7). In the cold-moist upper reaches, the $\delta^2\text{H}$ offset of trees, shrubs, and grasses showed significant negative correlations with temperature and positive correlations with relative humidity, with the response rate followed as grass ($-0.701\text{‰}/^\circ\text{C}$ and $0.149\text{‰}/\%$), shrub ($-0.672\text{‰}/^\circ\text{C}$ and $0.132\text{‰}/\%$) and tree ($-0.380\text{‰}/^\circ\text{C}$ and $0.087\text{‰}/\%$) (Fig. S6a,b). These results further revealed the $\delta^2\text{H}$ offset dependence on both temperature and relative humidity, indicating the degree of ^2H fractionation of herbaceous plants has the fastest response to temperature and relative humidity, followed by shrubs and trees under cold-moist environment. The reasons need to be further studied. In the middle reaches, the weak effects of temperature and relative humidity on the $\delta^2\text{H}$ offsets (Figs 4a,b, S6a,b) revealed the $\delta^2\text{H}$ offset's dependence on temperature and relative humidity decreasing gradually under the dry environments. For the lower reaches, the weak relationship between $\delta^2\text{H}$ offset of trees and relative humidity ($P < 0.05$) (Figs S5a,b, S6a,b) implied the complex effects of temperature and relative humidity on ^2H fractionation under extreme dry conditions. Considering these correlation patterns along the entire basin, we proposed that climate conditions imposed stronger influences on the plant water source $\delta^2\text{H}$ offsets than plant functional type.

Linkages between transpiration demand and plant water source $\delta^2\text{H}$ offset

Leaf water becomes enriched in the heavy isotopes ^2H and ^{18}O compared to the water entering the roots as a result of transpiration (Gonfiantini *et al.*, 1965). Therefore, we used observations of leaf water $\delta^{18}\text{O}_{\text{leaf}}$ and difference of leaf water $\delta^{18}\text{O}$ and xylem water $\delta^{18}\text{O}$ ($\Delta^{18}\text{O}_{\text{Leaf-xylem}}$) to explore the connections between the $\delta^2\text{H}$ offset and plant transpiration demand (Figs 3c,d, 4c,d, S3c,d, S4c,d, S5c,d, S6c,d).

On the basin and reach scales, the significantly negative correlations between $\delta^2\text{H}$ offsets and $\delta^{18}\text{O}_{\text{leaf}}/\Delta^{18}\text{O}_{\text{Leaf-xylem}}$ across the entire basin (Fig. S3c,d) and in the upper reaches (Fig. 4c,d) revealed that the stronger ^{18}O enrichment in leaf water through transpiration, the stronger negative $\delta^2\text{H}$ fractionation (Larcher *et al.*, 2015; Barbeta *et al.*, 2020; Casa *et al.*, 2022; Ellsworth *et al.*, 2023). No significant correlations between the $\delta^2\text{H}$ offset with $\delta^{18}\text{O}_{\text{leaf}}/\Delta^{18}\text{O}_{\text{Leaf-xylem}}$ were found in the middle reaches with relatively dry conditions, while significantly positive correlations were found in the lower reaches (Fig. 4c,d), indicating high transpiration resulted in a more positive $\delta^2\text{H}$ offset under extremely hot-dry conditions. It is interesting that the reverse correlations of $\delta^2\text{H}$ offsets with $\delta^{18}\text{O}_{\text{leaf}}/\Delta^{18}\text{O}_{\text{Leaf-xylem}}$ were found in the upper reaches (negative) with a cold-moist environment and in the lower reaches (positive) with an extremely hot-dry environment (Fig. 4c,d). These results suggested that the substantial effect of climate on the $\delta^2\text{H}$ offset was achieved by affecting leaf transpiration. For example, temperature affects $\delta^2\text{H}$ offsets (significant negative relationship) likely through controlling leaf transpiration via vapor pressure deficit (i.e. usually vapor pressure deficit increases with increasing temperature) in the upper cold and wet environment (Larcher *et al.*, 2015; Barbeta *et al.*, 2020; Casa *et al.*, 2022; Ellsworth *et al.*, 2023). While in the lower reaches with an extremely hot-dry environment, low air humidity (low relative humidity and high vapor pressure deficit) drives plant transpiration accordingly (increased, even at a constant stomatal conductance) affecting the $\delta^2\text{H}$ offset.

Regarding plant functional types, the significantly negative correlations between $\delta^2\text{H}$ offset with $\delta^{18}\text{O}_{\text{leaf}}$ and $\Delta^{18}\text{O}_{\text{Leaf-xylem}}$ of trees and grasses at the basin scale (Figs 3c,d, S6c,d), and between $\delta^2\text{H}$ offset with $\delta^{18}\text{O}_{\text{leaf}}$ of trees and grasses, and with $\Delta^{18}\text{O}_{\text{Leaf-xylem}}$ of tree in the upper reaches (Figs S4c,d, S6c,d) suggested that strong transpiration results in the greater $\delta^2\text{H}$ offset. In the lower reaches, weak positive correlations between $\delta^2\text{H}$ offsets of shrubs with $\delta^{18}\text{O}_{\text{leaf}}$ ($P = 0.033$) and of trees with $\Delta^{18}\text{O}_{\text{Leaf-xylem}}$ ($P = 0.038$) (Figs S5c,d, S6c,d) implied that high temperature and low humidity environment affected ^2H fractionation by limiting transpiration. Thus, for plant functional type, the effect of transpiration on $\delta^2\text{H}$ offsets was affected by climatic conditions at both basin and reach scales.

The effects of multi-factors on plant water source $\delta^2\text{H}$ offsets

From the upper to middle to lower reaches, annual mean temperature ranges between -2.9°C and 8.9°C , and precipitation

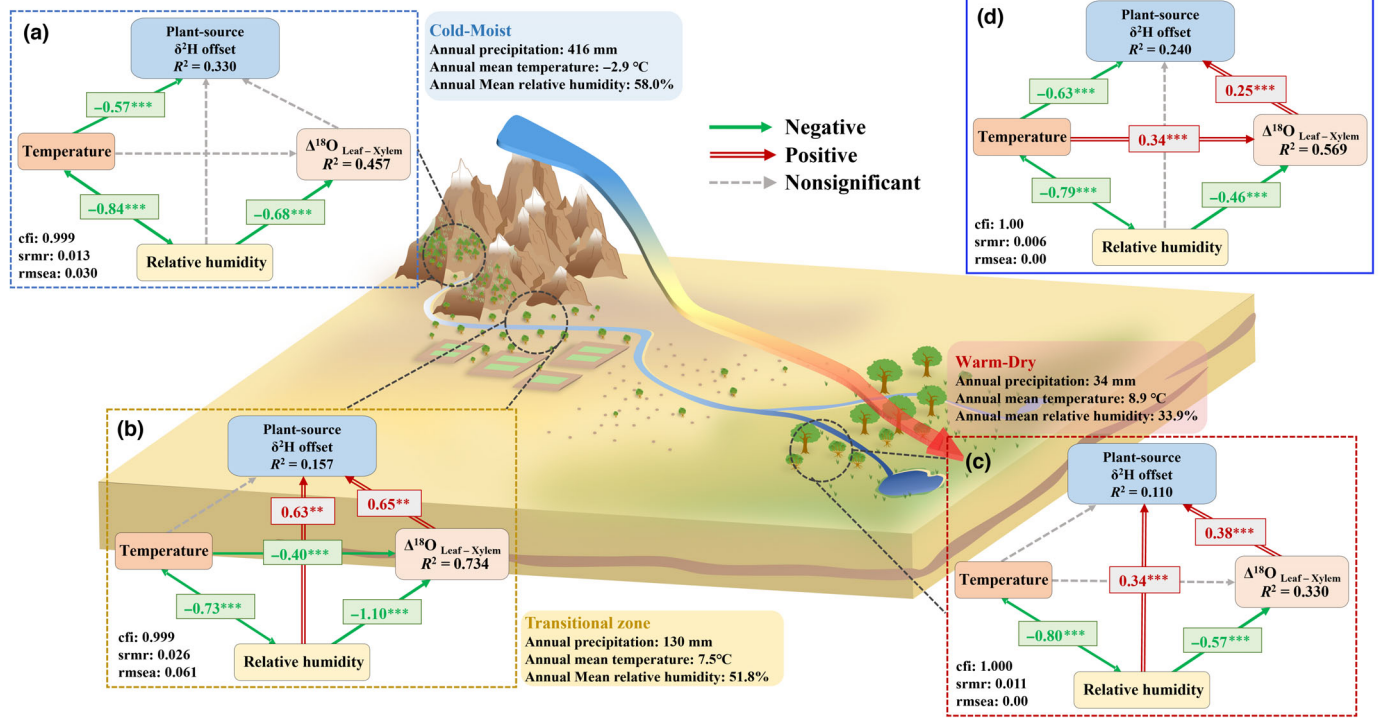


Fig. 5 Conceptual diagram showing the environmental background and potential contribution of climate factors on plant water source $\delta^2\text{H}$ offset across the inland Heihe River Basin. The averaged climate conditions are calculated based on the nearby meteorological stations covering the common period 1960–2012 (upper reaches, Yeniugou; middle reaches, Zhangye; lower reaches, Ejina). From the upper reaches to the lower reaches, the climate varies from cool-moist to warm-dry, which potentially impacts the $\delta^2\text{H}$ offset. The direct and indirect effects of climate and physiological parameters on plant water source $\delta^2\text{H}$ offset for the entire basin and each reach are depicted from the structure equation model (SEM). Continuous arrows indicate the relationships are significant at the $P \leq 0.05$. A dashed line indicates relationships are not significant. The double line arrows with dark red and green arrows indicate the positive and negative relationships, respectively. Numbers next to the paths indicate the effect size (standardized path coefficients, analogous to partial regression weights). Overall goodness-of-fit tests (Comparative Fit Index (cfi), Standardized Root Mean Square Residual (srmr), and Rooted Mean Square Error of Approximation (rmsea)) are shown to guarantee an acceptable fit at the left bottom of each model. In particular, $\delta^{18}\text{O}_{\text{leaf}}$ is not included in SEM due to co-varying with $\Delta^{18}\text{O}_{\text{leaf-xylem}}$. Panel (a), (b), (c), and (d) represent the upper, middle, lower, and entire basin, respectively. **, $P < 0.01$; ***, $P < 0.001$.

between 34 and 416 mm, respectively (Fig. 5). This indicates a strong climate gradient in thermo-moisture coupling stress on plant ecophysiological activities. To consider the potential linkages and interactions between climatic parameters, habitat, and plant transpiration, we used the Structural Equation Model (SEM) to evaluate the linkages between plant water source $\delta^2\text{H}$ offsets and each parameter (i.e. temperature, relative humidity, and $\Delta^{18}\text{O}_{\text{Leaf-Xylem}}$) at the basin and reach scales. The SEM analyses revealed that there were varied relationships between climate, $\Delta^{18}\text{O}_{\text{Leaf-Xylem}}$, and $\delta^2\text{H}$ offsets under different climatic conditions and different spatial scales. If we use $\Delta^{18}\text{O}_{\text{Leaf-Xylem}}$ as a measure of transpiration, plant leaf transpiration is primarily driven by temperature and air humidity, resulting in the hydrogen isotopic fractionation under different climatic conditions (Fig. 5). Only temperature impacted the $\delta^2\text{H}$ offsets significantly and positively (the higher the temperature, the more negative $\delta^2\text{H}$ offsets) in the upper reaches (Fig. 5a). Both $\Delta^{18}\text{O}_{\text{Leaf-Xylem}}$ (positive relationship) and $\delta^2\text{H}$ offsets (negative relationship) were affected by temperature at the basin scale (Fig. 5d). However, in the middle and lower reaches, both $\Delta^{18}\text{O}_{\text{Leaf-Xylem}}$

(negative relationship) and $\delta^2\text{H}$ offsets (positive relationship) were affected by relative humidity, and positive correlations of $\Delta^{18}\text{O}_{\text{Leaf-Xylem}}$ and $\delta^2\text{H}$ offsets with relative humidity were found (Fig. 5b,c). In addition, negative relationships between $\Delta^{18}\text{O}_{\text{Leaf-Xylem}}$ and relative humidity were found in the entire basin, the upper, middle, and lower reaches (Fig. 5a–d). Our results revealed that the effects of temperature and relative humidity on $\Delta^{18}\text{O}_{\text{Leaf-xylem}}$ and $\delta^2\text{H}$ offsets varied with climate and spatial scales. Generally, increased temperature promotes plant leaf transpiration thereby increasing $\Delta^{18}\text{O}_{\text{Leaf-xylem}}$ (Cernusak *et al.*, 2022; Ellsworth *et al.*, 2023). An increase in the transpiration rate also leads to an increase in the $\delta^2\text{H}$ offset (Vargas *et al.*, 2017; Barbeta *et al.*, 2020), which was consistent with our results that temperature promotes plant leaf transpiration, then leads to the more negative $\delta^2\text{H}$ offsets in the upper reaches and the entire basin scales under the conditions where temperature is the main impacting factor. In the middle and lower reaches, similar patterns that linked the relative humidity/ $\Delta^{18}\text{O}_{\text{Leaf-Xylem}}$ and $\delta^2\text{H}$ offsets were revealed, with stronger effects on the $\delta^2\text{H}$ offsets in the lower reaches under the extremely arid environment

(Fig. 5b,c). Relative humidity may have two ways to alter the $\delta^2\text{H}$ offsets: one is the positive direct linkage between relative humidity and the $\delta^2\text{H}$ offsets, and another is that it can alter the $\Delta^{18}\text{O}_{\text{Leaf-xylem}}$ through the regulation of transpiration by dynamic adjustment in stomata conductance and leaf water $\delta^{18}\text{O}$ (Cernusak *et al.*, 2022). In an extremely arid environment such as the middle and lower reaches, the linkages between relative humidity, the $\delta^2\text{H}$ offsets, and $\Delta^{18}\text{O}_{\text{Leaf-xylem}}$ were strong. This may be related to direct relative humidity control on transpiration, or impacts of relative humidity and temperature on transpiration, with respect to the $\Delta^{18}\text{O}_{\text{Leaf-xylem}}$ and $\delta^{18}\text{O}_{\text{Leaf water}}$ (Cernusak *et al.*, 2022). Previous studies also reported significantly positive relationships between transpirational water loss and isotope fractionation of soil–plant stem water for *Persea*

americana (Vargas *et al.*, 2017; Barbeta *et al.*, 2020), significant linear relationships between transpiration rate and oxygen isotope enrichment of leaf water above source water (Ellsworth *et al.*, 2023) and that leaf water $\delta^{18}\text{O}$ was more closely correlated with air relative humidity (Cernusak *et al.*, 2022). From the basin perspective, linkages between climates/ $\Delta^{18}\text{O}_{\text{Leaf-xylem}}$ and $\delta^2\text{H}$ offset represent the integrated features across the environmental gradient (Fig. 5d), masking the local spatial differences. It is possible that $\Delta^{18}\text{O}$ of ambient water vapor also influences the $\delta^2\text{H}$ offsets, and this influence requires future investigations. It also remains unclear what is the predominant bio-physical mechanism of the $\delta^2\text{H}$ offset, which is not only driven by environmental variables such as temperature and vapor pressure deficit/relative humidity but is also driven by plant characteristics, processes at

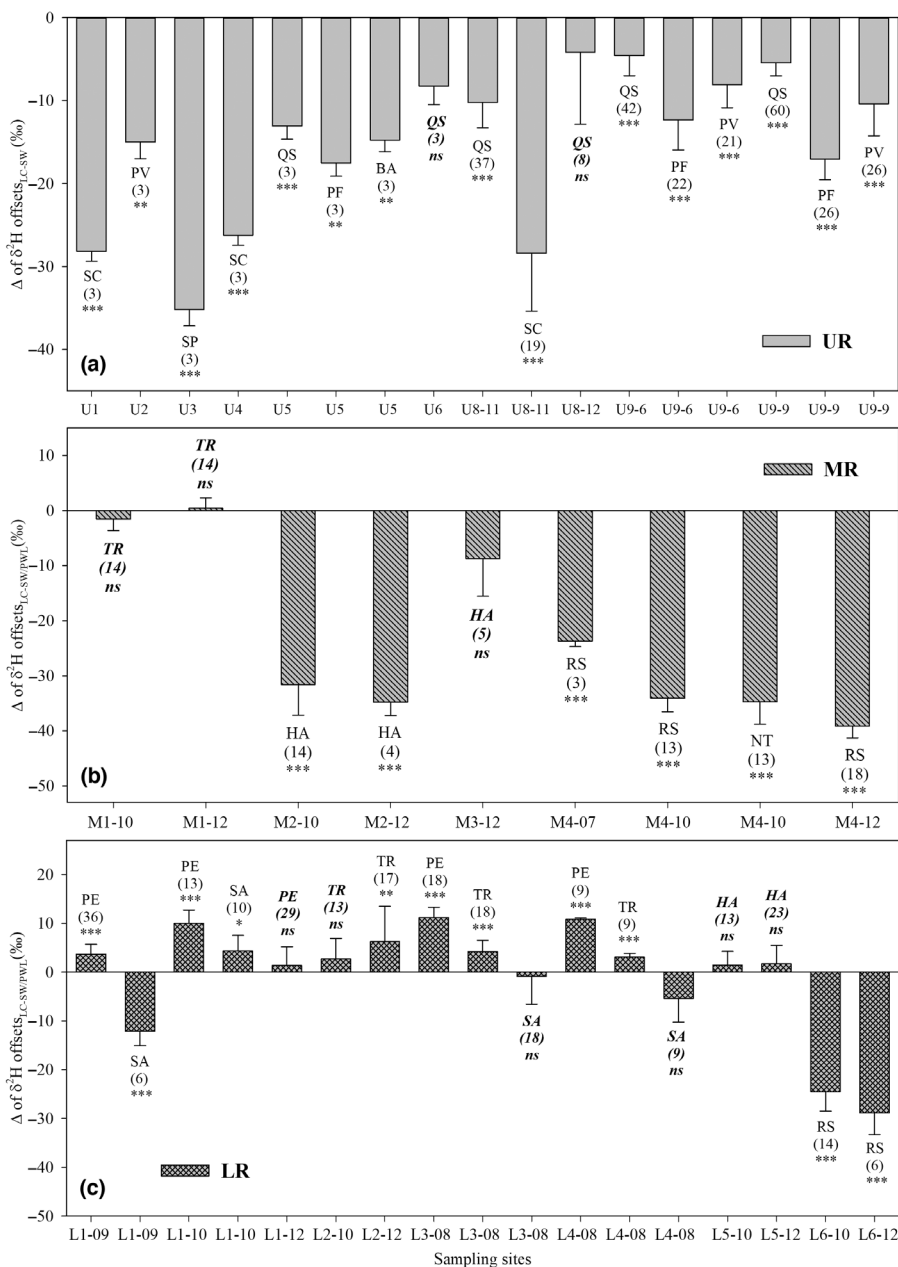


Fig. 6 Differences in $\delta^2\text{H}$ offsets between LC-excess and SW/PWL-excess calibration methods for upper reaches (UR) (a), middle reaches (MR) (b), and lower reaches (LR) (c). Δ of $\delta^2\text{H}$ offsets $_{\text{LC-SW}}$ indicates the plant potential water source is soil water. Δ of $\delta^2\text{H}$ offsets $_{\text{LC-PWL}}$ indicates the plant potential water sources are both soil water and groundwater. *, $P < 0.05$; **, $P < 0.01$; ***, $P < 0.001$; ns, nonsignificant. The SC, PV, SP, and SA indicate grasses *Stipa capillata* Linn, *Polygonum viviparum* L., *Stipa purpurea* Griseb and *Sophora alopecuroides*, respectively. PF, BA, RS, TR, HA and NT indicate shrubs *Potentilla fruticosa* L., *Berberis amurensis*, *Reaumuria soongorica* Maxim, *Tamarix ramosissima* Ledeb, *Haloxylon ammodendron* and *Nitraria tangutorum* Bobr, respectively. QS and PE indicate trees Qinghai Spruce and *Populus euphratica* Oliv, respectively. The error bars represent 1 SD.

the soil–root interface, the different degree of aquaporin mediated water transport in different species and the mixing of water sources in the plants. We noted that the total explained variance of climate and $\Delta^{18}\text{O}_{\text{Leaf-xylem}}$ in SEM results ranged from 11% of the lower reaches to 33% of the upper reaches (Fig. 5), suggesting that there is much room to clarify the detailed processes about the $\delta^2\text{H}$ offset occurring in plants growing along this natural climatic gradient. We thus recommend further investigations about ^2H isotope fractionation processes which are related to the species-specific metabolism and hydraulic drivers.

Implications of different correction methods to calculate plant water source $\delta^2\text{H}$ offsets

Assuming no ^{18}O fractionation To assess whether there was a hydrogen isotopic offset between plant water source and its potential sources ($\delta^2\text{H}$ offset) using different methods, the line-conditioned excess (LC-excess = $\delta^2\text{H} - a\delta^{18}\text{O} - b$) of Landwehr & Coplen (2004), the modified equation about SW-excess (Barbeta *et al.*, 2019) and PWL-excess (Li *et al.*, 2021) were proposed

assuming no oxygen isotopic fractionation occurs during root water uptake (Zhao *et al.*, 2016). Here we used the difference between LC-excess and the SW/PWL-excess (Δ of $\delta^2\text{H}$ offset LC-SW/PWL) to indicate the discrepancy. When plants only use soil water, the slope and intercept of SW-excess are lower than that of LMWL due to evaporation of soil water, and a more accurate offset value can be obtained by SW-excess correction (Fig. S8a). In addition, the differences between $\delta^2\text{H}$ offset-based LC-excess and $\delta^2\text{H}$ offset-based SW-excess are related to positive and negative fractionation occurrences (Fig. S8a). When plants use both soil water and groundwater, although there were significant differences between $\delta^2\text{H}$ offset-based LC-excess and $\delta^2\text{H}$ offset-based SW-excess, the $\delta^2\text{H}$ offset PWL-excess tended to be close to the $\delta^{18}\text{O}$ – $\delta^2\text{H}$ diagram of groundwater (Fig. S8b–g). This tendency is related to the position of the xylem water which is positioned above/below/on LC-excess in a $\delta^{18}\text{O}$ – $\delta^2\text{H}$ diagram (Fig. S8b–g). Our results also supported the best performance of the PWL-excess correction method (Li *et al.*, 2021). As shown in Fig. 6, except for two sites, compared with SW-excess, the correction results with LC-excess presented a significantly negative

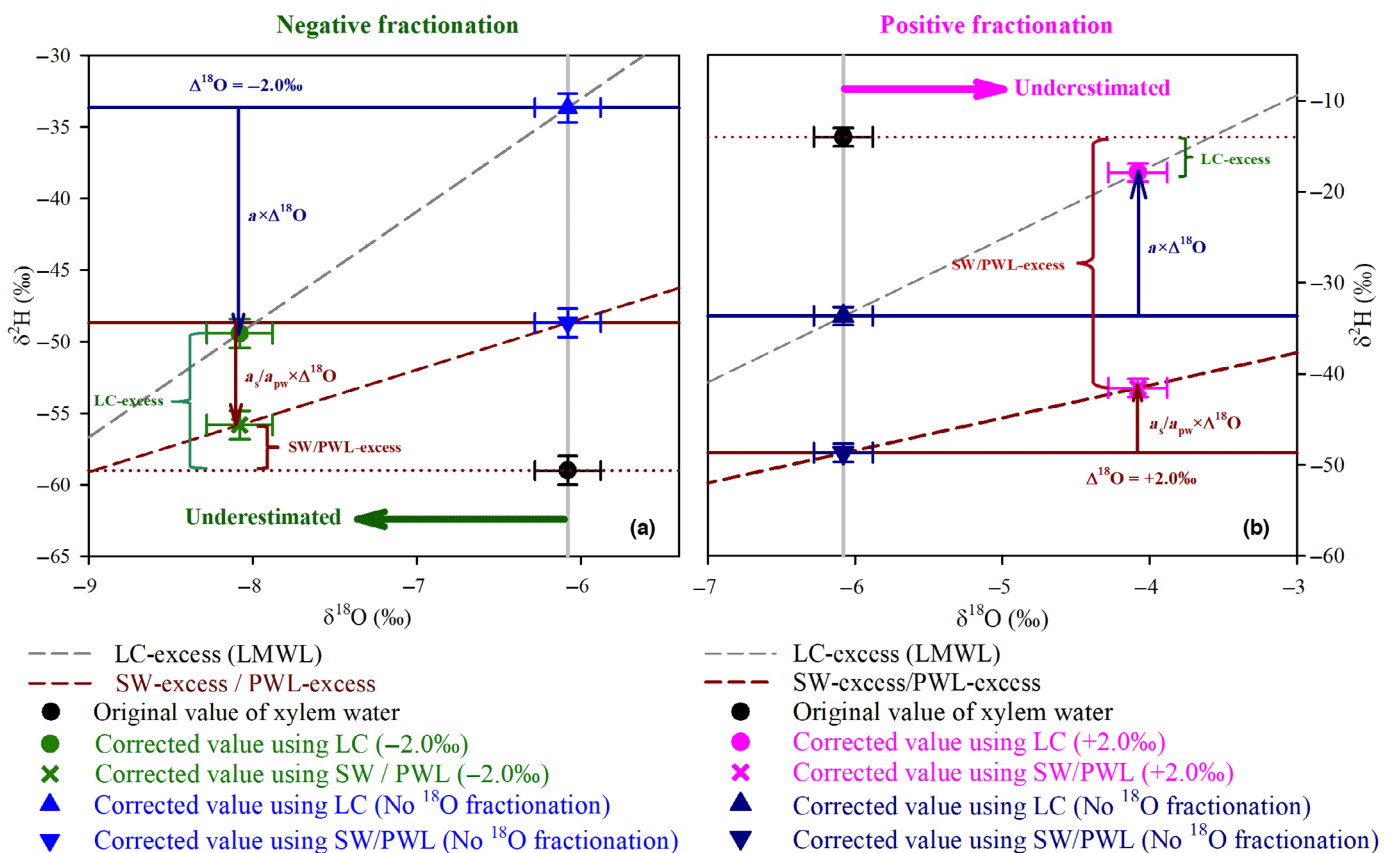


Fig. 7 The $\delta^2\text{H}$ offset assessment considering the negative (a) and positive (b) ^{18}O fractionation. Note: The numbers in the brackets indicate the corrected values by the two above methods when ^{18}O fractionations are -2 (a) and $+2$ (b) according to the results of Vargas *et al.* (2017), respectively. The LC-excess, SW-excess, and PWL-excess indicate the line-conditioned excess (LC-excess = $\delta^2\text{H} - a \times \delta^{18}\text{O} - b$, the a and b correspond to the slope and intercept of the LMWL, respectively), the soil water evaporated line (SW-excess = $\delta^2\text{H} - a_s \times \delta^{18}\text{O} - b_s$; the a_s and b_s are the slope and intercept of the soil water line for a given plot and date, respectively) and potential water source line (PWL-excess = $\delta^2\text{H} - a_{pw} \times \delta^{18}\text{O} - b_{pw}$; the a_{pw} and b_{pw} are the slope and intercept of the soil water and groundwater line for a given plot and date, respectively), respectively. The dark red and dark blue arrows represent $a_s/a_{pw} \times \Delta^{18}\text{O}$ and $a \times \Delta^{18}\text{O}$, respectively. The dark red and dark green brackets represent SW-excess and LC-excess, respectively. The error bars represent 1 SD.

deviation, with the maximum deviation (-35.2‰) found in the upper reaches (Fig. 6a). In the middle reaches, except for three sites, the same pattern was found with a maximum deviation of -39.2‰ (M4-12 for RS) (Fig. 6b). However, in the lower reaches, compared with SW-excess, LC-excess showed both positive deviation (11.2‰) and negative deviation (-28.8‰) (Fig. 6c). These results revealed that to obtain the true xylem water $\delta^2\text{H}$ values, we need to consider more potential water source to correct the hydrogen isotope fractionation in further studies.

Assuming ^{18}O fractionation For a non-xerophytic species, *Persea americana*, Vargas *et al.* (2017) reported that discrimination occurs against both ^2H and ^{18}O and concluded that the most plausible fractionation mechanisms occurred at the soil-root interface. They found that *Persea americana* plants discriminated against the heavier hydrogen isotopes *c.* 10 times more than oxygen isotopes during water uptake. This discrimination increased and depended on soil water loss, porosity, and particle size. According to the assessment of the $\delta^2\text{H}$ offset between plant xylem water and its potential sources such as $\text{LC-excess} = \delta^2\text{H} - a \times \delta^{18}\text{O} - b$ (Landwehr & Coplen, 2004), $\text{SW-excess} = \delta^2\text{H} - a_s \times \delta^{18}\text{O} - b_s$ (Barbeta *et al.*, 2019) and $\text{PWL-excess} = \delta^2\text{H} - a_{\text{pw}} \times \delta^{18}\text{O} - b_{\text{pw}}$ (Li *et al.*, 2021), if there is negative (Vargas *et al.*, 2017) or positive (this study) ^{18}O fractionation, the $\delta^2\text{H}$ offset were calculated by the slopes (a , a_s and a_{pw}) and $\Delta^{18}\text{O}$. It should be underestimated as $a \times \Delta^{18}\text{O}$, $a_s \times \Delta^{18}\text{O}$ and $a_{\text{pw}} \times \Delta^{18}\text{O}$ (Fig. 7). In order to eliminate the influence of ^{18}O fractionation, the $\delta^2\text{H}$ offsets should be calculated through $\text{LC-excess} = \delta^2\text{H} - a \times (\delta^{18}\text{O} + \Delta^{18}\text{O}) - b$, $\text{SW-excess} = \delta^2\text{H} - a_s \times (\delta^{18}\text{O} + \Delta^{18}\text{O}) - b_s$ and $\text{PWL-excess} = \delta^2\text{H} - a_{\text{pw}} \times (\delta^{18}\text{O} + \Delta^{18}\text{O}) - b_{\text{pw}}$ based on the previous methods in the future studies if ^{18}O fractionation was estimated (Fig. 7).

Concluding remarks

Building on an extensive field data set, this study identified negative, positive, or zero $\delta^2\text{H}$ offsets in different geographical environments, and confirmed that ^2H fractionation was a common phenomenon during water uptake via roots and subsequent redistributions. The degree of $\delta^2\text{H}$ offset depends on plant species, plant growth state, and climatic factors such as temperature and relative humidity. Different methods to correct $\delta^2\text{H}$ offset of stem water are performed differently under various water source conditions. In addition, our study suggests that methods used to correct the $\delta^2\text{H}$ offsets should consider the multiple potential water sources rather than the local meteoric water line alone. Our findings have significant implications for isotope-based ecohydrological and paleoclimate investigations.

Acknowledgements

This study was supported by the National Natural Science Foundation of China (Grant Nos. 42330501, 42271022, 41771028, and 41971104), the Second Tibetan Plateau Scientific Expedition and Research Program (2019QZKK020102), and the National Key Research and Development Program of China

(2017YFC0404302). We greatly appreciate the support and assistance of the Northwest Institute of Eco-Environment and Resources, Chinese Academy of Sciences.

Competing interests

None declared.

Author contributions

LZ designed the research, collected and measured the isotope data, and wrote the paper. XL collected and measured the isotope data. XL, NW, and LW wrote and revised the paper. AB developed the SEM models and revised the paper. LZ, XL AB, and YZ contributed to data analysis. LAC revised the manuscript. All authors commented on and edited the manuscript.

ORCID

Adrià Barbeta [ID https://orcid.org/0000-0002-8357-1719](https://orcid.org/0000-0002-8357-1719)
 Lucas A. Cernusak [ID https://orcid.org/0000-0002-7575-5526](https://orcid.org/0000-0002-7575-5526)
 Xiaohong Liu [ID https://orcid.org/0000-0002-1497-6122](https://orcid.org/0000-0002-1497-6122)
 Lixin Wang [ID https://orcid.org/0000-0003-0968-1247](https://orcid.org/0000-0003-0968-1247)
 Ninglian Wang [ID https://orcid.org/0000-0002-3612-1141](https://orcid.org/0000-0002-3612-1141)
 Yu Zhang [ID https://orcid.org/0000-0001-5324-7224](https://orcid.org/0000-0001-5324-7224)
 Liangju Zhao [ID https://orcid.org/0000-0001-7445-3916](https://orcid.org/0000-0001-7445-3916)

Data availability

The data that support the findings of this study are available in the [Supporting Information](#).

References

- Allen ST, Kirchner JW, Braun S, Siegwolf RTW, Goldsmith GR. 2019. Seasonal origins of soil water used by trees. *Hydrology and Earth System Sciences* 23: 1199–1210.
- Allen ST, Sprenger M, Bowen GJ, Brooks JR. 2022. Spatial and temporal variations in plant source water: O and H isotope ratios from precipitation to xylem water. In: Siegwolf RTW, Brooks JR, Roden J, Saurer M, eds. *Stable isotopes in tree rings. Tree physiology*. Cham, Switzerland: Springer, 501–535.
- Barbeta A, Burlett R, Martín-Gómez P, Frejaville B, Devert N, Wingate L, Domec JC, Ogee J. 2022. Evidence for distinct isotopic compositions of sap and tissue water in tree stems: consequences for plant water source identification. *New Phytologist* 233: 1121–1132.
- Barbeta A, Gimeno TE, Clavé L, Frejaville B, Jones SP, Delvigne C, Wingate L, Ogee JM. 2020. An explanation for the isotopic offset between soil and stem water in a temperate tree species. *New Phytologist* 227: 766–779.
- Barbeta A, Penuelas J. 2017. Relative contribution of groundwater to plant transpiration estimated with stable isotopes. *Scientific Reports* 7: 10580.
- Barbeta A, SamP J, Clavé L, Wingate L, Gimeno TE, Frejaville B, Wohl S, Ogee J. 2019. Unexplained hydrogen isotope offsets complicate the identification and quantification of tree water sources in a riparian forest. *Hydrology and Earth System Sciences* 23: 1–31.
- Casa J, Barbeta A, Rodríguez-Uña A, Wingate L, Ogee J, Gimeno TE. 2022. Isotopic offsets between bulk plant water and its sources are larger in cool and wet environments. *Hydrology and Earth System Sciences* 26: 4125–4146.
- Cernusak LA, Barbeta A, Bush RT, Eichstaedt (Bögelein) R, Ferrio JP, Flanagan LB, Gessler A, Martín-Gómez P, Hirl RT, Kahmen A *et al.* 2022. Do ^2H and

- ¹⁸O in leaf water reflect environmental drivers differently? *New Phytologist* 235: 41–51.
- Cernusak LA, Farquhar GD, Pate JS. 2005. Environmental and physiological controls over oxygen and carbon isotope composition of Tasmanian blue gum, *Eucalyptus globulus*. *Tree Physiology* 25: 129–146.
- Chen Y, Helliker BR, Tang X, Li F, Zhou YP, Song X. 2020. Stem water cryogenic extraction biases estimation in deuterium isotope composition of plant source water. *Proceedings of the National Academy of Sciences, USA* 117: 33345–33350.
- Dawson TE, Pate JS. 1996. Seasonal water uptake and movement in root systems of Australian phreatophytic plants of dimorphic root morphology: a stable isotope investigation. *Oecologia* 107: 13–20.
- Deurwaerder HD, Hervé-Fernández P, Stahl C, Burban B, Petronelli P, Hoffman B, Bonal D, Boeckx P, Verbeeck H. 2018. Liana and tree below-ground water competition—evidence for water resource partitioning during the dry season. *Tree Physiology* 38: 1–13.
- Diao HY, Schuler P, Goldsmith GR, Siegwolf RTW, Saurer M, Lehmann MM. 2022. Technical note: On uncertainties in plant water isotopic composition following extraction by cryogenic vacuum distillation. *Hydrology and Earth System Sciences* 26: 5835–5847.
- Ehleringer JR, Dawson TE. 1992. Water uptake by plants: perspectives from stable isotope composition. *Plant, Cell & Environment* 15: 1073–1082.
- Ehleringer JR, Roden JS, Dawson TE. 2000. Assessing ecosystem-level water relations through stable isotope ratio analysis. In: Sala O, Jackson R, Mooney H, eds. *Methods in ecosystem science*. New York, NY, USA: Springer, 181–198.
- Ellsworth PZ, Ellsworth PV, Mertz RA, Koteyeva NK, Cousins AB. 2023. Leaf cell wall properties and stomatal density influence oxygen isotope enrichment of leaf water. *Plant, Cell & Environment* 23: 1–17.
- Ellsworth PZ, Williams DG. 2007. Hydrogen isotope fractionation during water uptake by woody xerophytes. *Plant and Soil* 291: 93–107.
- Evaristo J, Jasechko S, McDonnell JJ. 2015. Global separation of plant transpiration from groundwater and streamflow. *Nature* 525: 91–94.
- Evaristo J, McDonnell JJ, Clemens J. 2017. Plant source water apportionment using stable isotopes: a comparison of simple linear, two-compartment mixing model approaches. *Hydrological Processes* 31: 3750–3758.
- Geris J, Tetzlaff D, McDonnell JJ, Soulsby C. 2017. Spatial and temporal patterns of soil water storage and vegetation water use in humid northern catchments. *Science of the Total Environment* 595: 486–493.
- Gonfiantini R, Gratziu S, Tongiorgi E. 1965. Oxygen isotope composition of water in leaves. In: *Isotopes and radiation in soil-plant nutrition studies*. Vienna, Austria: International Atomic Energy Agency.
- Jasechko S, Sharp ZD, Gibson JJ, Birks SJ, Yi Y, Fawcett PJ. 2013. Terrestrial water fluxes dominated by transpiration. *Nature* 496: 347–350.
- Landwehr JM, Coplen TB. 2004. Line-conditioned excess: a new method for characterizing stable hydrogen and oxygen isotope ratios in hydrologic systems. In: *Proceedings of an international conference held in Monaco. Isotopes in environmental studies*. Vienna, Austria: International Atomic Energy Agency, 132–135.
- Lanning M, Wang LX, Benson M, Zhang Q, Novick KA. 2020. Canopy isotopic investigation reveals different water uptake dynamics of maples and oaks. *Phytochemistry* 175: 112389.
- Larcher L, Hara-Nishimura I, Sternberg L. 2015. Effects of stomatal density and leaf water content on the ¹⁸O enrichment of leaf water. *New Phytologist* 206: 141–151.
- Li Y, Ma Y, Song X, Wang LX, Han DM. 2021. A $\delta^2\text{H}$ offset correction method for quantifying root water uptake of riparian trees. *Journal of Hydrology* 593: 125811.
- Lin GH, Sternberg LSL. 1992. Comparative study of water uptake and photosynthetic gas exchange between scrub and fringe red mangroves, *Rhizophora mangle* L. *Oecologia* 90: 399–403.
- Newberry SL, Nelson DB, Kahmen A. 2017. Cryogenic vacuum artifacts do not affect plant water-uptake studies using stable isotope analysis. *Ecology* 10: e1892.
- Oerter EJ, Bowen GJ. 2019. Spatio-temporal heterogeneity in soil water stable isotopic composition and its ecohydrologic implications in semiarid ecosystems. *Hydrological Processes* 33: 1724–1738.
- Peng TR, Liu KK, Wang CH, Chuang KH. 2011. A water isotope approach to assessing moisture recycling in the Island-based precipitation of Taiwan: a case study in the western Pacific. *Water Resources Research* 47: W08507.
- R Core Team. 2022. *A language and environment for statistical computing*. Vienna, Austria: R Foundation for Statistical Computing. [WWW document] URL <https://www.R-project.org> [accessed 22 April 2022].
- Renée Brooks J, Barnard HR, Coulombe R, McDonnell JJ. 2009. Ecohydrologic separation of water between trees and streams in a Mediterranean climate. *Nature Geoscience* 3: 100–104.
- Rosseel Y. 2012. LAVAAN: an R package for structural equation modeling. *Journal of Statistical Software* 48: 1–36.
- Sprenger M, Leister H, Gimbel K, Weiler M. 2016. Illuminating hydrological processes at the soil-vegetation-atmosphere interface with water stable isotopes. *Reviews of Geophysics* 54: 674–704.
- Vargas AI, Schaffer B, Yuhong L, Sternberg LDL. 2017. Testing plant use of mobile and immobile soil water sources using stable isotope experiment. *New Phytologist* 215: 582–594.
- Wang J, Fu BJ, Lu N, Zhang L. 2017. Seasonal variation in water uptake patterns of three plant species based on stable isotopes in the semi-arid Loess Plateau. *Science of the Total Environment* 609: 27–37.
- Wang LX, Caylor KK, Villegas JC, Barron-Gafford GA, Breshears DD, Huxman TE. 2010. Partitioning evapotranspiration across gradients of woody plant cover: assessment of a stable isotope technique. *Geophysical Research Letters* 37: L09401.
- Wang LX, Good SP, Caylor KK. 2014. Global synthesis of vegetation control on evapotranspiration partitioning. *Geophysical Research Letters* 41: 6753–6757.
- Wang LX, Good SP, Caylor KK, Cernusak LA. 2012. Direct quantification of leaf transpiration isotopic composition. *Agricultural and Forest Meteorology* 154: 127–135.
- Wang LX, Niu SL, Good SP, Soderberg K, McCabe MF, Sherry RA, Luo Y, Zhou X, Xia J, Caylor KK. 2013. The effect of warming on grassland evapotranspiration partitioning using laser-based isotope monitoring techniques. *Geochimica et Cosmochimica Acta* 111: 28–38.
- West AG, Goldsmith GR, Brooks PD, Dawson TE. 2010. Discrepancies between isotope ratio infrared spectroscopy and isotope ratio mass spectrometry for the stable isotope analysis of plant and soil waters. *Rapid Communications in Mass Spectrometry* 24: 1948–1954.
- West AG, Patrickson SJ, Ehleringer JR. 2006. Water extraction times for plant and soil materials used in stable isotope analysis. *Rapid Communications in Mass Spectrometry* 20: 1317–1321.
- Zhao LJ, Liu XH, Wang NL, Kong YL, Song YX, He ZB, Liu QY, Wang LX. 2019. Contribution of recycled moisture to local precipitation in the inland Heihe River Basin. *Agricultural and Forest Meteorology* 271: 316–335.
- Zhao LJ, Wang LX, Cernusak LA, Liu XH, Xiao HL, Zhou MX, Zhang SQ. 2016. Significant difference in hydrogen isotope composition between xylem and tissue water in *Populus euphratica*. *Plant, Cell & Environment* 39: 1848–1857.
- Zhao LJ, Xiao HL, Zhou J, Wang LX, Cheng GD, Zhou MX, Yin L, McCabe MF. 2011. Detailed assessment of isotope ratio infrared spectroscopy and isotope ratio mass spectrometry for the stable isotope analysis of plant and soil waters. *Rapid Communications in Mass Spectrometry* 25: 3071–3082.
- Zhao LJ, Xie C, Liu XH, Wang NL, Yu Z, Dong XY, Wang LX. 2020. Water sources of major plant species along a strong climatic gradient in the inland Heihe River Basin. *Plant and Soil* 455: 439–466.

Supporting Information

Additional Supporting Information may be found online in the Supporting Information section at the end of the article.

Fig. S1 Map showing the general environment of inland Heihe River Basin, distribution of sampling sites, and monthly climate parameters.

Fig. S2 The $\delta^{18}\text{O}$ - $\delta^2\text{H}$ isotope plots of xylem water and plant potential water sources across the Heihe River Basin.

Fig. S3 Influences of temperature, relative humidity, $\delta^{18}\text{O}_{\text{Leaf}}$ and $\Delta^{18}\text{O}_{\text{Leaf-xylem}}$ on $\delta^2\text{H}$ offset of plants.

Fig. S4 Transpiration sensitivity of $\delta^2\text{H}$ offset dependent on the plant function types in the upper reaches.

Fig. S5 Transpiration sensitivity of $\delta^2\text{H}$ offset dependent on the plant function types in the lower reaches.

Fig. S6 Sensitivity of plant water source $\delta^2\text{H}$ offsets to climate and transpiration at different scales.

Fig. S7 Relationships between temperature and air relative humidity during the sampling period.

Fig. S8 The schematic diagram of different corrected methods to attain $\delta^2\text{H}$ offset.

Methods S1 Additional field sampling details.

Please note: Wiley is not responsible for the content or functionality of any Supporting Information supplied by the authors. Any queries (other than missing material) should be directed to the *New Phytologist* Central Office.